

Anomaly Detection based on Markov Data: A Statistical Depth Approach

Carlos Fernández*

Stephan Cléménçon†

Abstract

The main purpose of this article is to extend the notion of statistical depth to the case of sample paths of a Markov chain. Initially introduced to define a center-outward ordering of points in the support of a multivariate distribution, depth functions permit to generalize the notions of quantiles and (signed) ranks for observations in \mathbb{R}^d with $d > 1$, as well as statistical procedures based on such quantities. In this paper, overcoming the lack of natural order on the torus composed of all possible trajectories of finite length, we develop a general theoretical framework for evaluating the depth of a Markov sample path and recovering it statistically from an estimate of its transition probability with (non-) asymptotic guarantees. We also detail some of its numerous applications, focusing particularly on anomaly detection, a key task in various fields involving the analysis of (supposedly) Markov time-series (*e.g.* health monitoring of complex infrastructures, security). Beyond the description of the methodology promoted and the statistical analysis carried out to guarantee its validity, numerical experiments are displayed, providing strong empirical evidence of the relevance of the novel concept we introduce here to quantify the degree of abnormality of Markov path sequences of variable length.

1 Introduction

The concept of Markov chain provides a very popular time-series model, ubiquitous in applications (*e.g.* systems engineering, bioinformatics, mathematical finance, operations research) to describe the dynamics governing the evolution of random time phenomena in a parsimonious way, namely systems with a past, whose future distribution depends on the most recent part only.

This paper is devoted to the extension of the *statistical depth* concept, originally introduced by [69] to overcome the lack of natural order on \mathbb{R}^d as soon as $d \geq 2$ and define quantiles for multivariate probability distributions as well as order and (signed) rank statistics (see *e.g.* [54]), to sample paths with variable length of a Markov chain $\mathbf{X} = (X_n)_{n \in \mathbb{N}}$. Whereas recent alternative approaches for curve/functional data are essentially based on topological/metric properties of

the path space (see *e.g.* [45, 66, 34]) and generally produce too large quantile regions when applied to Markov data as will be shown later, the framework we develop is tailored to the Markov setting. It relies on the description of the law of a Markov chain by its transition probability kernel, and can be seen as a very natural extension of the multivariate case.

Given a statistical depth on the state space, we propose to define the depth of a sample path as the geometric average of the depth of each state involved in it w.r.t. the transition probability evaluated at the preceding state. We show that the depth on the torus of all finite length trajectories thus constructed, inherits all the properties that the multivariate depth may enjoy, has significant computational advantages compared to its competitors and can be interpreted in a very intuitive fashion: the greater the average number of deep transitions, the deeper the path.

The accuracy of sampling versions of the Markov depth promoted is rigorously established in the form of (non-) asymptotic upper confidence bounds in the spirit of generalization guarantees in statistical learning theory. While such results have been mainly established under the assumption that training examples are i.i.d. (see *e.g.* [22]), the case of observations with a dependency structure, time-series in particular, has been the subject of intensive study in recent years, see for instance [1], [4], [67], [35] [68], [42], [23] or [3] among many others. Most of these works established (non-) asymptotic results assessing the generalization capacity of empirical risk minimization techniques or the accuracy of model selection methods based on time-series. These results mainly rely on extensions of probabilistic bounds for uniform deviations of i.i.d. averages from their expectation to the case of *weakly dependent training data*, under general assumptions related to the decay rate of *mixing coefficients*, see [63]. However, few works, with the exception of [18] for instance, are specific to the case of Markov chains and exploit their specific dynamics as we do in this paper.

Several promising applications related to the statistical analysis of Markov paths of variable lengths are also discussed. Motivated by practical problems in various domains (*e.g.* health monitoring, quality control, security), particular attention is paid to the task of de-

*LTCI, Télécom Paris, Institut Polytechnique de Paris.

†LTCI, Télécom Paris, Institut Polytechnique de Paris.

pecting abnormal trajectories. In the numerical experiments that have been carried out, the proposed methodology performs significantly better than pre-existing approaches, paving the way for its use in a wider range of tasks.

The paper is structured as follows. In section 2, the main notions of statistical depth are briefly recalled alongside the elements of Markov chain theory involved in the subsequent analysis. In section 3 we first introduce the concept of *Markovian depth function* which extends the idea of depth functions to the space of finite length paths of a Markov chain. Next we explain how to construct Markovian depth functions based on statistical depths defined on the state space and we study its main theoretical and statistical properties. Various numerical experiments illustrating the relevance of the concept we propose are presented in section 4. Section 5 collects a few concluding remarks and perspectives for further research, while, due to space limitations, all technical proofs as well as additional discussions, examples and applications are postponed to the Supplementary Material.

2 Background and Preliminaries

As a first go, we briefly recall some basic notions pertaining to statistical depth theory and key concepts in the study of Markov chains (refer to *e.g.* [53, 26] for a more detailed account), which shall be used in the paper. Throughout the article, we denote by $\mathbb{I}\{B\}$ the indicator function of any event B , by δ_a the Dirac mass at any point a and by \Rightarrow convergence in distribution. The Euclidean inner product and norm on \mathbb{R}^d are denoted by $\langle \cdot, \cdot \rangle$ and $\|\cdot\|$.

2.1 Statistical Depth Given the lack of any “natural order” on \mathbb{R}^d when $d \geq 2$, the notion of *statistical depth* allows to define a center-outward ordering of points in the support of a probability distribution P on \mathbb{R}^d and, as a result, to extend the notions of order and (signed) rank statistics to multivariate data, see [54]. By *depth function* relative to P is meant a function that determines the centrality of any point $x \in \mathbb{R}^d$ with respect to the probability measure P , that is to say any bounded non-negative Borel-measurable function $D_P : \mathbb{R}^d \rightarrow \mathbb{R}_+$ such that the points $x \in \mathbb{R}^d$ near the ‘center’ of the mass are the deepest (*i.e.* such that $D_P(x)$ is among the highest values taken by the function). The depth D_P thus enables us to define a preorder for multivariate points $x \in \mathbb{R}^d$. Originally introduced in the seminal contribution [69], the *half-space depth* of x in \mathbb{R}^d relative to P is the minimum of the measure $P(\mathcal{H})$ taken over all closed half-spaces $\mathcal{H} \subset \mathbb{R}^d$ such that $x \in \mathcal{H}$. Many alternatives have been developed, see *e.g.* [47], [41], [13], [59], [71]

or [16] among others. Refer to A1 in the Supplementary Material for a list of popular statistical depths for multivariate distributions and a discussion about computational issues. In [73], an axiomatic nomenclature of statistical depths has been devised, providing a systematic way of comparing their merits and drawbacks. Precisely, the four properties below should be ideally satisfied for any distribution on \mathbb{R}^d (see [28] and [54] for a different, though statistically equivalent, formulation).

- (P1) (AFFINE INVARIANCE) Meaning by P_X the distribution of any r.v. X valued in \mathbb{R}^d , it holds: $D_{P_{AX+b}}(Ax + b) = D_P(x)$ for all $x \in \mathbb{R}^d$, any r.v. X taking its values in \mathbb{R}^d , any $d \times d$ nonsingular matrix A with real entries and any vector b in \mathbb{R}^d .
- (P2) (VANISHING AT INFINITY) For any probability distribution P on \mathbb{R}^d , the depth function D_P vanishes at infinity, *i.e.* $D_P(x) \rightarrow 0$ as $\|x\|$ tends to infinity.
- (P3) (MAXIMALITY AT CENTER) For any probability distribution P on \mathbb{R}^d possessing a symmetry center x_P (in a sense to be specified), the depth function D_P takes its maximum value at it, *i.e.* $D_P(x_P) = \sup_{x \in \mathbb{R}^d} D_P(x)$.
- (P4) (MONOTONICITY RELATIVE TO THE DEEPEST POINT) For any distribution P on \mathbb{R}^d with deepest point x_P , the depth at any point x in \mathbb{R}^d decreases as one moves away from x_P along any ray passing through it, *i.e.* $D_P(x) \leq D_P(x_P + \alpha(x - x_P))$ for any α in $[0, 1]$.

Several studies have examined whether some of the properties listed above are verified by the various notions of statistical depth proposed in the literature, see *e.g.* [73]. Questions of a different nature have also been investigated. One can refer to [61] for computational aspects, see also *e.g.* [29] for algorithms related to Tukey’s halfspace depth. The continuity properties of the depths, in both x and P , have also been studied for most statistical depths, see *e.g.* [24, 72, 57].

As the distribution P of interest is usually unknown in practice, its analysis must rely on the observation of $N \geq 1$ independent realizations X_1, \dots, X_N of P . A statistical version of $D_P(x)$ can be built by replacing P with an empirical counterpart \hat{P}_N based on the X_i ’s, *e.g.* the raw empirical distribution $(1/N) \sum_{i=1}^N \delta_{X_i}$, to get the *empirical depth function* $D_{\hat{P}_N}(x)$. The consistency and asymptotic normality of empirical depth functions have been analyzed for different notions of statistical depth, refer to *e.g.* [24] and [72], and concentration results for empirical half-space depth and contours can be found in [11] and [9]. The ranks and order statistics derived from a depth function can be used for

a variety of tasks, *e.g.* classification [46], clustering [39], anomaly detection [56] or two-sample tests [65] among others. The case of functional data has received some attention in the literature. Although most practical approaches consist in projecting first the functional data onto an appropriate finite dimensional space (*filtering*) and using next a notion of multivariate depth, certain methods recently documented rely on metrics or exploit the geometry of the trajectories/curves in the path space, see [45, 66, 34]. As will be shown in the subsequent analysis, such techniques perform poorly when applied to Markov data, given the possibly great dispersion of Markov probability laws. In contrast to the methodology we propose, none of them exploits the underlying Markov dynamics/structure of the sample paths and is suitable to analyze trajectories of different lengths.

2.2 Basic Properties of Markov Chains We first recall a few definitions concerning the communication structure and the stochastic stability of Markov chains. Let $\mathbf{X} = (X_n)_{n \in \mathbb{N}}$ be a (time-homogeneous) Markov chain (of order 1) defined on some probability space $(\Omega, \mathcal{F}, \mathbb{P})$ with a countably generated state space $E \subseteq \mathbb{R}^d$ equipped with its Borel σ -field $\mathcal{B}(E)$, transition probability kernel $\Pi : (x, A) \in E \times \mathcal{B}(E) \mapsto \Pi_x(A)$ and initial probability distribution ν . For any $A \in \mathcal{B}(E)$ and $n \in \mathbb{N}$, we thus have that $X_0 \sim \nu$ and

$$(2.1) \quad \mathbb{P}(X_{n+1} \in A \mid X_0, \dots, X_n) = \Pi_{X_n}(A) \quad a.s.$$

We denote by \mathbb{P}_ν (respectively, by \mathbb{P}_x for x in E) the probability measure on the underlying probability space such that $X_0 \sim \nu$ (resp. $X_0 = x$) and by $\mathbb{E}_\nu[\cdot]$ the \mathbb{P}_ν -expectation (resp. by $\mathbb{E}_x[\cdot]$ the \mathbb{P}_x -expectation).

The chain \mathbf{X} is said to be *irreducible* if there exists a σ -finite measure ψ s.t. for all set $B \in \mathcal{B}(E)$, when $\psi(B) > 0$, the chain visits B with strictly positive probability, no matter what the starting point is. Assuming ψ -irreducibility, there is $d \in \mathbb{N}^*$ and disjoint sets A_1, \dots, A_d ($A_{d+1} = A_1$) weighted by ψ such that $\psi(E \setminus \bigcup_{1 \leq i \leq d} A_i) = 0$ and $\forall x \in A_i$, $\Pi(x, A_{i+1}) = 1$. The greatest common divisor of such integers is the *period* of the chain \mathbf{X} , which is said *aperiodic* when it equals 1.

A Borel set A is *Harris recurrent* for the chain \mathbf{X} if for any $x \in A$, $\mathbb{P}_x(\sum_{n=1}^{\infty} \mathbb{I}\{X_n \in A\} = \infty) = 1$. The chain \mathbf{X} is said *Harris recurrent* if it is ψ -irreducible and every measurable set A s.t. $\psi(A) > 0$ is Harris recurrent. When the chain is Harris recurrent, we have the property that $\mathbb{P}_x(\sum_{n=1}^{\infty} \mathbb{I}\{X_n \in A\} = \infty) = 1$ for any $x \in E$ and any $A \in \mathcal{B}(E)$ such that $\psi(A) > 0$. A probability measure μ on E is said invariant for \mathbf{X} when $\mu\Pi = \mu$, where $\mu\Pi(dy) = \int_{x \in E} \mu(dx)\Pi_x(dy)$.

An irreducible chain is said *positive recurrent* when it admits an invariant probability (it is then unique).

EXAMPLE 2.1. (MODULATED RANDOM WALK) Consider the model defined by $X_0 = x_0 \geq 0$ and $X_{n+1} = \max(0, X_n + W_n)$ for $n \in \mathbb{N}$ where (W_n) is a sequence of i.i.d. random variables with distribution F . Then, X_n is a Markov chain on $E = [0, \infty)$ with transition kernel: $\Pi(x, [0, y]) = F(y-x) \quad x, y \geq 0$. When $\mathbb{E}[W_1] < 0$, the chain is positive recurrent [53, Proposition 11.4.1]. Such a modulated random walk on the half-line models various systems, such as content-dependent storage processes, work-modulated single server queues, see e.g. [5, Section III.6].

Denote by $\mathbb{T} = \bigcup_{n \geq 1} E^n$ the torus of all trajectories of finite length in the state space E , equipped with its usual topology $\mathcal{T} = \{O \subset \mathbb{T} : \forall n \geq 1, O \cap E^n \in \mathcal{B}(E^n)\}$ (see [27, pp. 131] or Section A2 of the Supplementary Material for further details). Any observed finite length trajectory (x_0, \dots, x_n) of \mathbf{X} is an element of \mathbb{T} . Our goal is to develop tools for assessing the *centrality*, or the *outlyingness* conversely, of elements of \mathbb{T} w.r.t. the distribution of a Markov chain \mathbf{X} . As illustrated in the example below, classic path depths based on the geometry of the space of trajectories are inappropriate even in the simple case where all trajectories have the same length.

EXAMPLE 2.2. (LIMITS OF GEOMETRIC APPROACHES) Consider the model described in Example 2.1, where $W_n = -1.1 \times Y_n + 1$ and the Y_n 's are i.i.d. exponential r.v.'s with mean 1. Note that, with probability 1: $W_n \leq 1$, hence $X_{n+1} - X_n \leq 1$. Fig. 1a shows, in solid red line, an unfeasible trajectory $\mathbf{x} = (0, x_1, \dots, x_5)$ where $x_2 - x_1 = 1.1$, sandwiched between two feasible trajectories (green/orange dashed lines). We have calculated the Lens and Mahalanobis depths (MBD) of this unfeasible trajectory w.r.t. the joint probability distribution of X_1, \dots, X_5 , obtaining the values 0.42 and 0.097 respectively, very close to the depths of the feasible ones that surround it in Fig. 1b and 1c..

3 Depth functions for Markov Chains

This section is devoted to extending the concept of statistical depth function to the domain of Markov chains. We propose a very general mechanism for constructing such Markov depth functions and then investigate their main properties. Particular attention is paid to the study of sampling versions.

3.1 Markovian Depth Functions As stated in the introduction, our goal is to extend the notion of depth

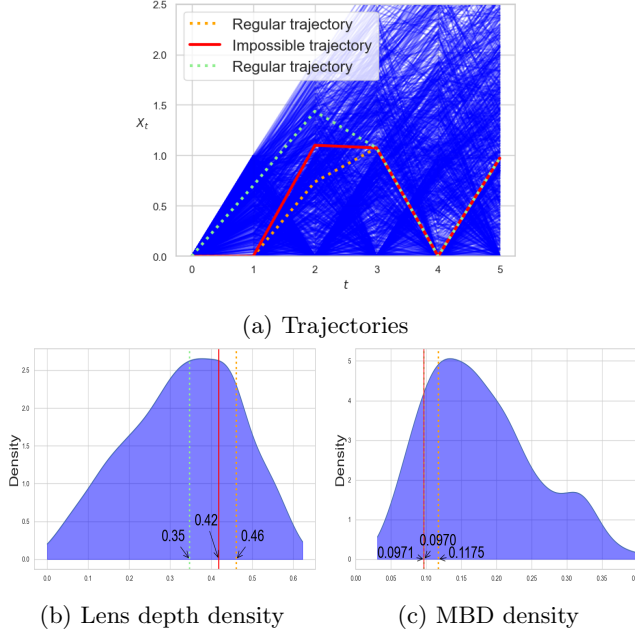


Figure 1: (a) an unfeasible trajectory (red line) of the modulated random walk on the half-line surrounded by two regular trajectories (green and orange dotted lines). (b) and (c), the densities of Lens and Mahalanobis depths w.r.t. the joint distribution of X_1, \dots, X_5 .

function to the space \mathbb{T} of finite length trajectories of a Markov chain in order to assess the centrality or outlyingness of Markov paths. The following is a list of a priori desirable properties for such functions on \mathbb{T} .

DEFINITION 3.1. (MARKOVIAN DEPTH FUNCTION) *A statistical depth function w.r.t. the distribution of the Markov chain \mathbf{X} is a function $\mathbf{D}_{\mathbf{X}} : \mathbb{T} \rightarrow \mathbb{R}_+$ that may satisfy some of the following properties:*

(M0) (INDEPENDENCE FROM THE INITIAL LAW) *If \mathbf{X} and \mathbf{X}' are two Markov chains with the same transition kernel, then: $\forall \mathbf{x} \in \mathbb{T}$,*

$$\mathbf{D}_{\mathbf{X}}(\mathbf{x}) = \mathbf{D}_{\mathbf{X}'}(\mathbf{x}).$$

(M1) (AFFINE INVARIANCE) *For any $d \times d$ non singular matrix A and $b \in \mathbb{R}^d$, it holds that: $\forall \mathbf{x} \in \mathbb{T}$,*

$$\mathbf{D}_{A\mathbf{X}+b}(A\mathbf{x} + b) = \mathbf{D}_{\mathbf{X}}(\mathbf{x}),$$

where we set $A\mathbf{x} + b = (Ax_0 + b, \dots, Ax_n + b)$ when $\mathbf{x} = (x_0, \dots, x_n)$.

(M2) (VANISHING AT INFINITY) *We have $\mathbf{D}_{\mathbf{X}}(\mathbf{x}) \rightarrow 0$ as \mathbf{x} “tends to infinity” in the sense \mathbb{T} ’s topology \mathcal{T} .*

Property (M0) in the above definition guarantees that the depth only depends on the dynamics, *i.e.* the transition probability kernel Π , which can be easily estimated with (non-) asymptotic guarantees based on the observation of a single Markov path of sufficiently long length $N \geq 1$ (see *e.g.* [17] and [40] and the references therein). Properties (M1) and (M2) are the natural extensions of the properties (P1) and (P2) of the depth functions on E to the path space \mathbb{T} . Regarding the extension of property (P3), though symmetry centers can be defined in the path space in certain (seldom) situations, they do not necessarily correspond to realizable paths, as illustrated in section A4 of the Supplementary Material, in which case the maximality at center property is absolutely not desirable. Notice also that, because of the absence of any vector space structure on \mathbb{T} , there is no natural equivalent to the monotonicity property (P4) in the Markovian case.

In the next subsection we propose a simple and efficient way to build Markovian depth functions on \mathbb{T} based on statistical depth functions on E .

3.2 Markovian Sample Path Depth Consider any notion of statistical depth D on E and let $\mathbf{x} = (x_0, \dots, x_n)$ be a finite length realization of the chain \mathbf{X} with initial distribution ν and kernel Π . For any $i \in \{1, \dots, n\}$, x_i is a realization of the transition probability $\Pi_{x_{i-1}}$, a distribution on E , and its depth can be naturally quantified through $D_{\Pi_{x_{i-1}}}(x_i)$. As formulated below, we propose to define the depth of the path \mathbf{x} by aggregating the depth of all transitions forming the path \mathbf{x} , as the geometric mean of the depths of each state transition.

DEFINITION 3.2. (MARKOVIAN SAMPLE PATH DEPTH) *With the convention that $\sqrt[0]{0} = 0$ for $n \geq 1$, the Markov depth function of a chain \mathbf{X} with transition Π based on the multivariate statistical depth D is the real-valued function defined on the torus \mathbb{T} of all trajectories of finite length as: $\forall n \geq 1, \forall \mathbf{x} = (x_0, \dots, x_n) \in E^{n+1}$,*

$$(3.2) \quad D_{\Pi}(\mathbf{x}) = \sqrt[n]{\prod_{i=1}^n D_{\Pi_{x_{i-1}}}(x_i)}.$$

When none of the $D_{\Pi_{x_{i-1}}}(x_i)$ ’s is 0, it can be written as $D_{\Pi}(\mathbf{x}) = \exp((1/n) \sum_{i=1}^n \log(D_{\Pi_{x_{i-1}}}(x_i)))$.

This definition extends that of statistical depth for multivariate distributions. Indeed, when $n = 1$, we have $D_{\Pi}((x_0, x_1)) = D_{\Pi_{x_0}}(x_1)$. The rationale behind it is obvious: *the deeper in average the transitions forming the path, the deeper the trajectory*. In particular, if

an impossible transition $x_{i-1} \rightarrow x_i$ is present in the trajectory \mathbf{x} (i.e. $D_{\Pi_{x_{i-1}}}(x_i) = 0$), its Markov depth equals 0, i.e. $D_{\Pi}(\mathbf{x}) = 0$. Provided that the depth functions D_{Π_x} can be easily computed (or estimated, see the analysis below), the Markovian sample path depth permits to evaluate and compare the depth of paths of any (finite) length.

EXAMPLE 3.1. (MARKOVIAN HALF-SPACE DEPTH) *If the Markov depth is based on the half-space depth introduced in [69] (see also section A1.1 in the Supplementary Material), it takes the form: $\forall n \geq 1, \forall \mathbf{x} = (x_0, \dots, x_n) \in E^{n+1}$,*

$$(3.3) \quad D_{\Pi}(\mathbf{x}) = \sqrt[n]{\prod_{i=1}^n \inf_{u \in \mathbb{S}_{d-1}} \Pi_{x_{i-1}}(\mathcal{H}_{u, x_i})},$$

where $\mathcal{H}_{u, x} = \{y \in \mathbb{R}^d : \langle u, y - x \rangle \geq 0\}$ for all $(u, x) \in \mathbb{S}_{d-1} \times E$.

In addition to its interpretability, the concept introduced has a number of advantages, as it inherits many properties from the notion of multivariate statistical depth it relies on (see Theorems 3.1, 3.2 and 3.3). As discussed in the following, the choice of D must be weighed against the verification of the desirable properties and the availability of efficient algorithms for computation in the case of empirical distributions (i.e. for computing $D_{\hat{P}}$, where \hat{P} is a statistical version of the distribution P considered).

Main Properties. Before investigating at length the theoretical properties of the Markovian sample path depth and inference issues, we state the following result, revealing that the Markov depth of a positive recurrent chain \mathbf{X} , evaluated at a random path of length $n+1$, is *stochastically stable* as $n \rightarrow \infty$, meaning that its distribution asymptotically converges to a Gaussian limit as the path length n increases.

PROPOSITION 3.1. (LIMIT DISTRIBUTION) *Assume that \mathbf{X} is positive recurrent with stationary distribution μ and that $\log(D_{\Pi_x}(y))$ is integrable w.r.t. $\mu d(x) \Pi_x(dy)$ in E^2 . Then, for any initial distribution ν , we have $D_{\Pi}(X_0, X_1, \dots, X_n) \rightarrow D_{\infty}(\Pi) \mathbb{P}_{\nu}$ almost-surely as $n \rightarrow \infty$, where*

$$(3.4) \quad D_{\infty}(\Pi) = \exp \left(\int_{(x,y) \in E^2} \log(D_{\Pi_x}(y)) \Pi_x(dy) \mu(dx) \right).$$

If in addition $\log(D_{\Pi_x}(y))$ is square integrable w.r.t. $\mu d(x) \Pi_x(dy)$, then we have that, as n goes to ∞ ,

$$\sqrt{n} \left(D_{\Pi}(X_0, X_1, \dots, X_n) - D_{\infty}(\Pi) \right)$$

converges in distribution to a centered normal random variable. The exact form of the asymptotic variance is given by (A6.6) in the Supplementary Material.

Our next result shows that the Markovian sample path depth D_{Π} inherits most of its statistical properties from the multivariate depth D it is based on, and for most choices of D , it satisfies the properties given in Definition 3.1.

THEOREM 3.1. *Let D be a statistical depth on E and D_{Π} be the Markovian sample path depth based on the latter. The following assertions hold true.*

- (i) *The Markovian depth D_{Π} satisfies (M0).*
- (ii) *If D satisfies (P1), then D_{Π} satisfies (M1).*
- (iii) *Assume that D fulfills the following stronger version of property (P2): $\forall M > 0$, $\sup_{\|x\| \leq M} D_{\Pi_x}(y) \rightarrow 0$ as $\|y\| \rightarrow \infty$. Then D_{Π} satisfies (M2).*

In addition to the above properties, D_{Π} also satisfies the following property, which can be viewed as a variation of (P3).

PROPOSITION 3.2. (MAXIMALITY AT PATHS OF CENTERS) *Let Π be a transition probability on \mathbb{R}^d . Assume that D fulfills property (P3) for a given notion of symmetry, that the distribution $\Pi_x(dy)$ on E is 'symmetric' w.r.t. a center $\theta(x) \in E$ for any $x \in E$ and that $x \in E \mapsto D_{\Pi_x}(\theta(x))$ is constant. Then, for any initial value $x_0 \in \mathbb{R}^d$ and any $n \geq 1$, the trajectory $(x_0, \theta^{(1)}(x_0), \dots, \theta^{(n-1)}(x_0))$ is of maximal Markov depth D_{Π} , where $\theta^{(1)}(x_0) = \theta(x_0)$ and $\theta^{(i+1)}(x_0) = (\theta \circ \theta^{(i)})(x_0)$ for $i \geq 1$.*

We point out that the paths considered in Proposition 3.2 above are not symmetry centers for \mathbf{X} 's law in general.

Continuity (in \mathbf{x} , in Π). The following classic technical conditions are involved in the subsequent study of the continuity properties of the Markov depth.

(P5) (CONTINUITY IN x) For any law P on \mathbb{R}^d , the mapping $x \in \mathbb{R}^d \mapsto D_P(x)$ is continuous.

(P6) (UNIFORM WEAK CONTINUITY IN P) For any probability distributions P and P_n on \mathbb{R}^d s.t. $P_n \Rightarrow P$ as $n \rightarrow \infty$, we have $\sup_{x \in \mathbb{R}^d} |D_{P_n}(x) - D_P(x)| \rightarrow 0$ as $n \rightarrow \infty$.

(P6') (WEAK CONTINUITY IN P) For any probability distributions P and P_n on \mathbb{R}^d s.t. $P_n \Rightarrow P$ as $n \rightarrow \infty$, we have: $\forall x \in \mathbb{R}^d, |D_{P_n}(x) - D_P(x)| \rightarrow 0$ as $n \rightarrow \infty$.

(P7) (WEAK FELLER CONDITION) Denoting by $\mathcal{M}_1(E)$ the set of probability measures on E equipped with the weak convergence topology, the function $x \in E \mapsto \Pi_x$ mapping E to $\mathcal{M}_1(E)$ is continuous.

Properties (P5) and (P6) are satisfied by many notions of statistical depth, see section A1. The result below reveals that the Markov depth inherits its continuity properties from those of the multivariate depth D involved in its definition.

THEOREM 3.2. *The following assertions hold true.*

- (i) (CONTINUITY IN \mathbf{x}) *Suppose that properties (P5), (P6) and (P7) are fulfilled. Then, the mapping $\mathbf{x} \in \mathbb{T} \mapsto D_{\Pi}(\mathbf{x})$ is continuous.*
- (ii) (CONTINUITY IN Π) *Suppose that (P6') is fulfilled. Let Π and $\Pi^{(n)}$ be transition probabilities on E s.t. $\forall x \in E, \Pi_x^{(n)} \Rightarrow \Pi_x$ as $n \rightarrow \infty$. Then: $\forall \mathbf{x} \in \mathbb{T}, D_{\Pi^{(n)}}(\mathbf{x}) \rightarrow D_{\Pi}(\mathbf{x})$.*

Sampling Versions and Estimation. The Markovian depth D_{Π} is unknown in general, just like the transition probability Π . In practice, a *plug-in* strategy based on an empirical counterpart $\hat{\Pi}$ of Π and must be implemented, using $D_{\hat{\Pi}}$ as an estimate of D_{Π} . Refer to A3 in the Supplementary Material for a description of inference techniques dedicated to the statistical estimation of Π with (non-asymptotic) guarantees. The following condition, which can be viewed as strong version of (P6), permits to link Π 's estimation error with that of D_{Π} .

(P6'') (LIPSCHITZ CONDITION) Let \mathcal{A} be a collection of Borel subsets of \mathbb{R}^d . There exists a finite constant C_d such that, for any probability distributions P and Q on \mathbb{R}^d , we have: $\sup_{x \in \mathbb{R}^d} |D_P(x) - D_Q(x)| \leq C_d \|P - Q\|_{\mathcal{A}}$, where $\|P - Q\|_{\mathcal{A}} := \sup_{A \in \mathcal{A}} |P(A) - Q(A)|$.

Property (P6'') is fulfilled by various multivariate depths for specific classes \mathcal{A} . For instance, it is fulfilled by the *simplicial depth* when $\mathcal{A} = \{\cap_{i=1}^d H_i : H_1, \dots, H_d$ open half-spaces of $\mathbb{R}^d\}$, see Dümbgen [30, Theorem 1]. As shown by the theorem below, non-asymptotic guarantees for sampling versions of the Markov depth can be established under this condition.

THEOREM 3.3. *Let $n \geq 1$ and $\mathbf{x} \in E^{n+1}$. Consider two transition probabilities Π and $\hat{\Pi}$ on E . Suppose that D fulfills (P6'') and $\exists \epsilon > 0$ s.t. $\min\{D_{\hat{\Pi}_i}(x_{i+1}), D_{\Pi_i}(x_{i+1})\} > \epsilon$ for $i < n$. We have*

$$(3.5) \quad |D_{\Pi}(\mathbf{x}) - D_{\hat{\Pi}}(\mathbf{x})| \leq \frac{7}{4} C_d \frac{D_{\Pi}(\mathbf{x})}{\epsilon} \max_{i=0, \dots, n-1} \|\Pi_{x_i} - \hat{\Pi}_{x_i}\|_{\mathcal{A}}$$

The above result deserves some comments. It proves that error bounds (in expectation, in probability) for point-wise deviations between $D_{\Pi}(\mathbf{x})$ and $D_{\hat{\Pi}}(\mathbf{x})$ can be straightforwardly deduced from bounds for the maximal deviations over the class \mathcal{A} between the transition probability Π_x and its estimator $\hat{\Pi}_x$ at the successive points x forming the path \mathbf{x} considered. In addition, as $\min_{1 \leq i < n} D_{\Pi_{x_{i-1}}}(x_i) \rightarrow 0$, the factor $D_{\Pi}(\mathbf{x})/\epsilon$ on the right hand side of (3.5) increases to ∞ , showing that the smaller the Markov depth value to be estimated with a given error bound, the higher the accuracy of the transition probability estimator required.

Computational issues. Various efficient algorithmic procedures have been designed to compute the values taken by a depth function in the multivariate case, based on a discrete, empirical distribution (see e.g. [55] and <https://data-depth.github.io>). The approach below shows how to use the latter to estimate the values taken by a Markovian sample path depth.

ALGORITHM 3.1. Estimation of $D_{\hat{\Pi}}(\mathbf{x})$.

Input: Path $\mathbf{x} = (x_0, \dots, x_n)$ with $n \geq 1$ in \mathbb{T} , transition probability $\hat{\Pi}$, and precision control integer $M \geq 1$

Output: Estimated Markov depth $D_{\hat{\Pi}}(\mathbf{x})$

1. For $i = 0$ to $n - 1$:

- (a) Generate M independent samples $x_{1,i}, \dots, x_{M,i}$ from $\hat{\Pi}_{x_i}$
- (b) Compute an estimator \hat{D}_i of $D_{\hat{\Pi}_{x_i}}(x_{i+1})$ based on $y_{1,i}, \dots, y_{M,i}$

2. Return $D_{\hat{\Pi}}(\mathbf{x}) = \sqrt[n]{\prod_{i=1}^n \hat{D}_i}$

Attention should be paid to the fact that the complexity of estimating the value that $D_{\hat{\Pi}}$ takes at a path of length $n + 1$ through Algorithm 3.1 is of order $O(ng(M, d))$, where $O(g(M, d))$ is the numerical complexity of computing the value taken by the empirical depth function $D_{\hat{P}}$ based on M independent samples of P . For instance, we have $g(M, d) = M^{d-1} \log M$ in the case of the half-space depth, see e.g. [50, 29]. In comparison, the complexity of calculating the value taken by the multivariate depth at (x_0, \dots, x_n) , viewed as a point of $\mathbb{R}^{(n+1)d}$, based on M paths of length $n + 1$ (viewed as M sample points in $\mathbb{R}^{(n+1)d}$) is of order $O(g(M, (n+1)d))$ (namely, $M^{(n+1)d-1} \log M$ in the case of the half-space depth). As a result, the Markov depth offers considerable computational advantages over the direct use of multivariate depth when considering “long” trajectories.

4 Application to Anomaly Detection

The proposed notion of Markov depth can be used for various tasks related to the statistical analysis of Markov paths of different lengths. For reasons of space and given the importance of this task in practice, the focus is on (unsupervised) anomaly detection in this section. Applications of the Markov depth to the clustering of Markov paths of different lengths and to the problem of testing whether two collections of Markov trajectories are drawn from the same (unknown) transition probability are described in the Supplementary Material, together with dedicated numerical experiments.

Unsupervised anomaly detection. Markov chains are used in a wide variety of fields, including systems engineering to model storage systems or tele-traffic data as well as time-series analysis, and (unsupervised) anomaly detection plays a crucial role in the monitoring/management of such complex systems/phenomena. Precisely, the problem considered is as follows. The objective is to identify paths \mathbf{x} that are suspicious due to their significant difference with the majority of observed sample paths. Here, an observation $\mathbf{x} = (x_0, \dots, x_n)$ with fixed length $n \geq 1$ and initial value $x_0 \in \mathbb{R}^d$ is *abnormal* when it is not the realization of the Markov chain with transition probability Π generating the *normal* (“not abnormal”, with no reference to the Gaussian law here) trajectories, *i.e.* when it is not a realization of the probability distribution $\delta_{x_0}(dx_0)\Pi(x_0, dy_1)\Pi(y_1, dy_2)\dots\Pi(y_{n-1}, dy_n)$, Π being unknown in practice of course. Based on a set of (unlabeled, but supposedly normal in vast majority) training paths, the goal is to build an anomaly scoring rule $s : \mathbb{T} \rightarrow \mathbb{R}$ permitting to assign a level of abnormality $s(\mathbf{x})$ to any future path \mathbf{x} in \mathbb{R} : the lower the score $s(\mathbf{x})$, the more suspicious the path \mathbf{x} observed ideally. Although the learning stage involves unlabeled datasets, the availability of labels is required to assess predictive performance (possibly depending on the type of anomaly considered). The gold standard in this respect is the ROC curve, *i.e.* the parameterized curve describing the rate of normal paths with a score below t (false positive rate) compared to that of abnormal paths with a score below t (true positive rate), as the t threshold varies, or its popular scalar summary, the AUC criterion (*i.e.* the Area Under the ROC Curve).

Below, we describe the two experimental contexts for which we then present the numerical results. The latter reveal that the performance of the simple method of using an empirical version of a Markov depth as the anomaly scoring function is quite similar to that of conventional techniques (which can only be used in contrast when the training/test paths are all of

the same length) when considering well-identified isolated/displacement/shape anomalies (see [36]) and significantly outperforms them when the anomaly is of a dynamic nature (*i.e.* corresponding to a more or less long-lasting change in transition dynamics), in line with its original motivation. This is confirmed by the additional experiments documented in the Supplementary Material.

Nonlinear time-series. Consider the ARCH(1) Markov chain, defined by: $X_{n+1} = m(X_n) + \sigma(X_n)\epsilon_n$ where $m : \mathbb{R} \mapsto \mathbb{R}$ and $\sigma : \mathbb{R} \mapsto \mathbb{R}_+^*$ are unknown measurable functions and ϵ_n is a sequence of i.i.d. r.v.’s with mean 0 and variance 1 independent of X_0 . Here, we have chosen $X_0 \equiv 0.5$, $m(x) = 1/(1 + \exp(-x))$ and $\sigma(x) = \psi(x+1.2) + 1.5\psi(x-1.2)$ where $\psi(x)$ is $\mathcal{N}(0, 1)$ ’s density function and $\epsilon_n \sim \mathcal{N}(0, 1)$.

Queuing system. Consider now a GI/G/1 queuing system with interarrival times T_n and service times V_n where $\{T_n\}_{n \geq 0}$ and $\{V_n\}_{n \geq 0}$ are independent i.i.d. sequences with distributions V and T respectively. Denote by X_n the waiting time of the n -th customer and assume that $X_0 = 0$, then, $X_{n+1} = \max(0, X_n + W_n)$ where $W_n = V_n - T_n$, which corresponds to Example 2.1. Here, V and T are exponential r.v.’s with means 0.45 and, 0.5 respectively.

Generation of anomalous paths. We examine 4 types of anomalies (isolated/shock, two dynamic and shift), generated by modifying the Markov model over a path segment. For the ARCH(1) model, the isolated anomaly is simulated by setting $m(x) = 5x$ and $\sigma(x) = |x|^{1/2}$ for two steps. The first dynamic anomaly alters $m(x) = 1/(2 + \exp(-x))$ for 60% of the path, while the second takes $\sigma(x) = 0.5\sqrt{x^2 + 1}$ over 60% of the trajectory. The shift anomaly uses $m(x) \equiv 2$ for 60% of the path length.

For the queuing system, the shock anomaly is generated by using V as an exponential distribution with a mean of 2.25 over 10% of the trajectory. The first dynamic anomaly changes the interarrival time distribution T to an exponential with a mean of 0.1 over 20% of the path, simulating a period of increased customer arrivals. The second dynamic anomaly modifies the service time distribution V to $0.55\mathcal{U}$, where \mathcal{U} is uniform on $(0, 2)$, over 30% of the path, representing a period of slightly slower service times. The shift anomaly is generated by considering deterministic interarrival times $T_n = 2^{-n}$ over 25 of steps. For more details on each anomaly and their generation, see B1.2.

For each model we simulated one long training path ($n = 1000$) and 4 contaminated data sets, each one containing 200 paths of random length (between 50 and 200) where 50% of those contain a specific type of

anomaly. Based on the long path, a kernel estimator $\hat{\Pi}$ (see A3) is computed and used to infer, for each trajectory, the Markov depth D_{Π} based on the half-space depth.

Results and Discussion. The results in Table 1 indicate that the Markov depth detects with high accuracy classic anomalies such as shocks/shifts, see Fig. 2a and 3b. Our approach is also capable of detecting the more challenging dynamic anomalies, see Fig. 2b and 3a. The corresponding ROC curves in Fig. 2 and 3 reveal its strong performance on the different types of anomaly considered. In Section B1.4, it is compared with that of alternative anomaly detection techniques, focusing on fixed-length paths since the competitors cannot straightforwardly handle variable-length paths. The results of these experiments, presented in Table 2 and Fig. 9 and 10 in the Supplementary Material, show that our method performs similarly to the best of the competitors for classic anomalies and significantly outperforms them for dynamic ones.

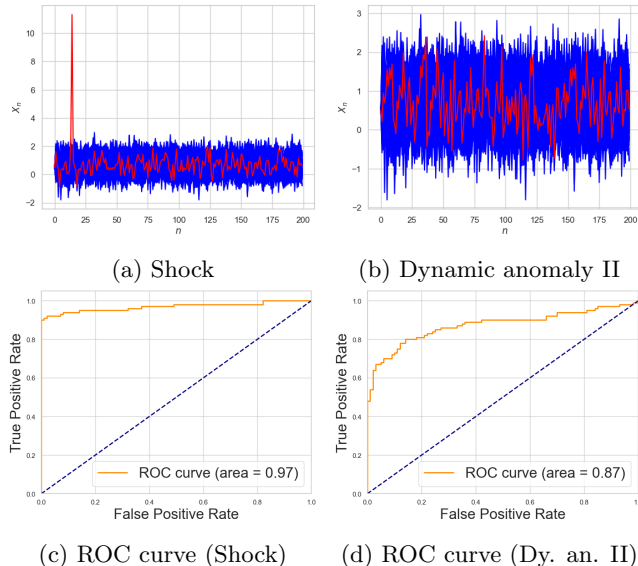


Figure 2: Subfigures (a) and (b) illustrate anomalies in the ARCH(1) model, with normal paths shown in blue and anomalous trajectories in red. Subfigures (c) and (d) present the ROC curves of our scoring function for the shock and dynamic anomaly II scenarios.

5 Some Concluding Remarks and Perspectives

In this paper, we have proposed a concept of statistical depth tailored to Markov data/laws, relying on classic approaches in the multivariate setting. A list of desirable properties have been shown to be satisfied when the Markov depth is based on popular choices for the un-

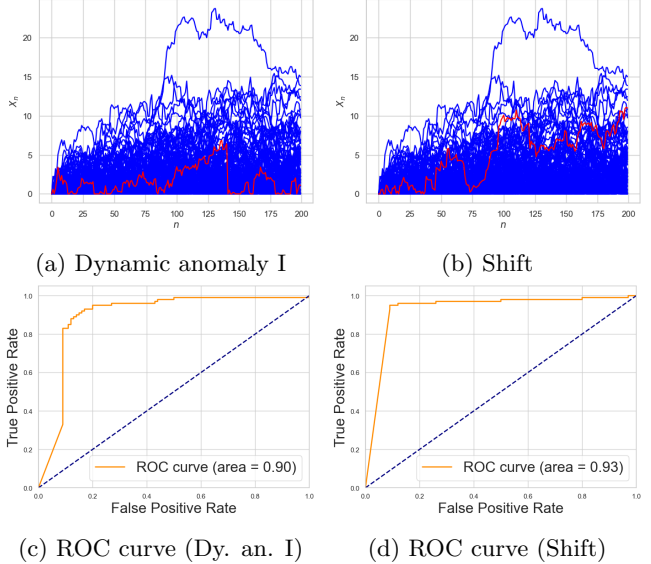


Figure 3: Subfigures (a) and (b) show anomalies in the queuing model: blue lines are normal paths and red lines are anomalous paths. Subfigures (c) and (d) display the ROC curves of our scoring function for these types of anomalies.

Table 1: AUC for each type of anomaly in the ARCH(1) and queuing models

Anomaly type	ARCH(1)	Queuing
Shock	0.97	0.95
Dynamic anomaly I	0.71	0.90
Dynamic anomaly II	0.87	0.73
Shift	1.00	0.93

derlying multivariate depth. The concept is promoted throughout the article as a very natural way of defining an ordering on the set of trajectories of variable (finite) length, so as to extend the notions of order statistics and ranks for Markov data. Theoretical and experimental results have also been presented in this article, showing that Markov depth can be accurately estimated by its empirical version and may serve to detect anomalous paths in a reliable manner. It may be used to perform a wide variety of other statistical tasks, ranging from the design of homogeneity tests between sets of trajectories of possibly different lengths to the clustering of Markov paths through the design of dedicated visualization techniques. Beyond the experiments we have presented here for illustrative purposes only, we plan to further investigate the suitability of this tool for the analysis of Markov data.

References

- [1] T. Adams and A. Nobel. Uniform convergence of VC classes under ergodic sampling. *Annals of Probability*, 38:1345–1367, 2010.
- [2] P. Afshani, D. R. Sheehy, and Y. Stein. Approximating the simplicial depth in high dimensions. In *The European Workshop on Computational Geometry*, 2016.
- [3] A. Agarwal and J. Duchi. The Generalization Ability of Online Algorithms for Dependent Data. *IEEE Transactions on Information Theory*, 59(1): 573–587, 2013.
- [4] P. Alquier and O. Wintenberger. Model selection for weakly dependent time series forecasting. *Bernoulli*, 18:883–913, 2012.
- [5] S. Asmussen. *Applied Probability and Queues*. Stochastic Modelling and FApplied Probability. Springer New York, New York, 2nd edition, 2010. ISBN 1441918094.
- [6] K. B. Athreya and G. S. Atuncar. Kernel estimation for real-valued markov chains. *Sankhyā: The Indian Journal of Statistics, Series A (1961-2002)*, 60(1):1–17, 1998. ISSN 0581572X.
- [7] A. K. Basu and D. K. Sahoo. On berry-esseen theorem for nonparametric density estimation in markov sequences. *Bulletin of Informatics and Cybernetics*, 1998.
- [8] T. Bollerslev, R. Y. Chou, and K. F. Kroner. Arch modeling in finance: A review of the theory and empirical evidence. *Journal of Econometrics*, 52, apr 1992. doi: 10.1016/0304-4076(92)90064-x.
- [9] V. E. Brunel. Concentration of the empirical level sets of tukey’s halfspace depth. *Probability Theory and Relative Fields*, 173:1165–1196, 2019.
- [10] P. S. Bullen. *A Dictionary of Inequalities*. CRC Press, 1 edition, 1998. ISBN 0582327482; 9780582327481.
- [11] M. A. Burr and R. J. Fabrizio. Uniform convergence rates for halfspace depth. *Statistics and Probability Letters*, 124:33–40, 2017.
- [12] M. A. Burr, E. Rafalin, and D. L. Souvaine. Simplicial depth: An improved definition, analysis, and efficiency for the finite sample case. In *CCCG*, pages 136–139, 2004.
- [13] P. Chaudhuri. On a geometric notion of quantiles for multivariate data. *Journal of the American Statistical Association*, 91(434):862–872, 1996.
- [14] D. Chen, P. Morin, and U. Wagner. Absolute approximation of tukey depth: Theory and experiments. *Computational Geometry*, 46(5):566–573, 2013. ISSN 0925-7721. doi: <https://doi.org/10.1016/j.comgeo.2012.03.001>. Geometry and Optimization.
- [15] A. Y. Cheng and M. Ouyang. On algorithms for simplicial depth. In *CCCG*, pages 53–56, 2001.
- [16] V. Chernozhukov, A. Galichon, M. Hallin, and M. Henry. Monge–kantorovich depth, quantiles, ranks and signs. *The Annals of Statistics*, 45(1): 223–256, 2017.
- [17] S. Clémenton. Adaptive estimation of the transition density of a regular Markov chain by wavelet methods. *Math. Meth. Statist.*, 9(4):323–357, 2000.
- [18] S. Clémenton, G. Ciolek, and P. Bertail. Statistical learning based on markovian data: Maximal deviation inequalities and learning rates. *The Annals of Mathematics and Artificial Intelligence*, 88, jan 2020.
- [19] S. Clémenton, P. Mozharovskyi, and G. Staerman. Affine invariant integrated rank-weighted statistical depth: properties and finite sample analysis. *Electronic Journal of Statistics*, 17(2):3854 – 3892, 2023. doi: 10.1214/23-EJS2189.
- [20] J. Cuesta-Albertos and A. Nieto-Reyes. The random tukey depth. *Computational Statistics and Data Analysis*, 52(11):4979–4988, 2008. ISSN 0167-9473.
- [21] A. Cuevas and R. Fraiman. On depth measures and dual statistics. a methodology for dealing with general data. *Journal of Multivariate Analysis*, 100 (4):753–766, 2009. ISSN 0047-259X.
- [22] L. Devroye, L. Györfi, and G. Lugosi. *A Probabilistic Theory of Pattern Recognition*. Springer, 1996.
- [23] J. Di and E. Kolaczyk. Complexity-penalized estimation of minimum volume sets for dependent data. *Journal of Multivariate Analysis*, 101(9): 1910–1926, 2004.
- [24] D. L. Donoho and M. Gasko. Breakdown properties of location estimates based on halfspace depth and projected outlyingness. *The Annals of Statistics*, 20:1803–1827, 1992.

[25] C. Dorea. Strong consistency of kernel estimators for markov transition densities. *Bulletin of the Brazilian Mathematical Society*, 33:409–418, 2002.

[26] R. Douc, E. Moulines, P. Priouret, and P. Soulier. *Markov chains*. Springer Series in Operations Research and Financial Engineering. Springer, 2018. ISBN 978-3-319-97704-1,3319977040,978-3-319-97703-4.

[27] J. Dugundji. *Topology*. Allyn and Bacon Series in Advanced Mathematics. Allyn and Bacon, 12th printing edition, 1978. ISBN 9780697068897; 0697068897.

[28] R. Dyckerhoff. Data depths satisfying the projection property. *Allgemeines Statistisches Archiv*, 88(2):163–190, 2004.

[29] R. Dyckerhoff and P. Mozharovskyi. Exact computation of the halfspace depth. *Computational Statistics and Data Analysis*, 98:19–30, 2016.

[30] L. Dümbgen. Limit theorems for the simplicial depth. *Statistics and Probability Letters*, 14, may 1992. doi: 10.1016/0167-7152(92)90075-g.

[31] R. T. Elmore, T. P. Hettmansperger, and F. Xuan. Spherical data depth and a multivariate median. *DIMACS Series in Discrete Mathematics and Theoretical Computer Science*, 72:87, 2006.

[32] R. F. Engle. Autoregressive conditional heteroscedasticity with estimates of the variance of united kingdom inflation. *Econometrica*, 50(4): 987–1007, 1982. ISSN 00129682, 14680262.

[33] J. Fan and Q. Yao. Efficient estimation of conditional variance functions in stochastic regression. *Biometrika*, 85(3):645–660, 1998. ISSN 00063444.

[34] G. Geenens, A. Nieto-Reyes, and G. Francisci. Statistical depth in abstract metric spaces. *Statistics and Computing*, 33(2):46, 2023.

[35] S. Hanneke. Learning whenever learning is possible: Universal learning under general stochastic processes. *arXiv:1706.01418*, 2017.

[36] M. Hubert, P. J. Rousseeuw, and P. Segaert. Multivariate functional outlier detection. *Statistical Methods & Applications*, 24(2):177–202, 2015.

[37] W. Härdle and A. Tsybakov. Local polynomial estimators of the volatility function in nonparametric autoregression. *Journal of Econometrics*, 81(1): 223–242, 1997. ISSN 0304-4076.

[38] D. Johnson and F. Preparata. The densest hemisphere problem. *Theoretical Computer Science*, 6(1):93–107, 1978. ISSN 0304-3975.

[39] R. Jörnsten. Clustering and classification based on the l_1 data depth. *Journal of Multivariate Analysis*, 90(1):67–89, 2004.

[40] H. Karlsen and D. Tjøstheim. Nonparametric estimation in null recurrent time series. *The Annals of Statistics*, 29, 04 2001. doi: 10.1214/aos/1009210546.

[41] G. Koshevoy and K. Mosler. Zonoid trimming for multivariate distributions. *The Annals of Statistics*, 25(5):1998–2017, 1997.

[42] V. Kuznetsov and M. Mohri. Generalization Bounds for Time Series Prediction with Non-stationary Processes. In *Proceedings of ALT'14*, 2014.

[43] C. Lacour. Adaptive estimation of the transition density of a markov chain. *Annales de l'Institut Henri Poincaré (B) Probability and Statistics*, 43(5):571–597, 2007. ISSN 0246-0203.

[44] C. Lacour. Nonparametric estimation of the stationary density and the transition density of a markov chain. *Stochastic Processes and their Applications*, 118(2):232–260, 2008.

[45] P. Lafaye De Micheaux, P. Mozharovskyi, and M. Vimond. Depth for curve data and applications. *Journal of the American Statistical Association*, 2020.

[46] T. Lange, K. Mosler, and P. Mozharovskyi. Fast nonparametric classification based on data depth. *Statistical Papers*, 55(1):49–69, 2014.

[47] Liu. On a notion of data depth based upon random simplices. *The Annals of Statistics*, 18(1):405–414, 1990.

[48] R. Y. Liu and K. Singh. A quality index based on data depth and multivariate rank tests. *Journal of the American Statistical Association*, 88, mar 1993. doi: 10.2307/2290720.

[49] R. Y. Liu, J. M. Parelius, and K. Singh. Multivariate analysis by data depth: descriptive statistics, graphics and inference, (with discussion and a rejoinder by Liu and Singh). *The Annals of Statistics*, 27(3):783 – 858, 1999. doi: 10.1214/aos/1018031260.

[50] X. Liu and Y. Zuo. Computing halfspace depth and regression depth. *Communications in Statistics - Simulation and Computation*, 43(5):969–985, 2014. doi: 10.1080/03610918.2012.720744.

[51] Z. Liu and R. Modarres. Lens data depth and median. *Journal of Nonparametric Statistics*, 23(4):1063–1074, 2011. doi: 10.1080/10485252.2011.584621.

[52] P. C. Mahalanobis. On the generalized distance in statistics. In *Proceedings of the National Institute of Sciences of India*, volume 2, pages 49–55, 1936.

[53] S. Meyn, R. Tweedie, and P. Glynn. *Markov chains and stochastic stability*. Cambridge Mathematical Library. Cambridge University Press, 2 edition, 2009. ISBN 9780521731829, 0521731828.

[54] K. Mosler. Depth statistics. In C. Becker, R. Fried, and S. Kuhnt, editors, *Robustness and Complex Data Structures: Festschrift in Honour of Ursula Gather*, pages 17–34. Springer, 2013.

[55] K. Mosler and P. Mozharovskyi. Choosing among notions of multivariate depth statistics. *Statistical Science*, 37(3):348–368, 2022.

[56] P. Mozharovskyi. Anomaly detection using data depth: multivariate case, 2022.

[57] S. Nagy, I. Gijbels, M. Omelka, and D. Hlubinka. Integrated depth for functional data: statistical properties and consistency. *ESAIM: PS*, 20:95–130, 2016. doi: 10.1051/ps/2016005.

[58] S. Nagy, R. Dyckerhoff, and P. Mozharovskyi. Uniform convergence rates for the approximated halfspace and projection depth. *Electronic Journal of Statistics*, 14(2):3939 – 3975, 2020. doi: 10.1214/20-EJS1759.

[59] H. Oja. Descriptive statistics for multivariate distributions. *Statistics and Probability Letters*, 1(6):327–332, 1983.

[60] F. Pedregosa, G. Varoquaux, A. Gramfort, V. Michel, B. Thirion, O. Grisel, M. Blondel, P. Prettenhofer, R. Weiss, V. Dubourg, J. Vanderplas, A. Passos, D. Cournapeau, M. Brucher, M. Perrot, and E. Duchesnay. Scikit-learn: Machine learning in python. *Journal of Machine Learning Research*, 12:2825–2830, 2011. ISSN 1532-4435.

[61] O. Pokotylo, P. Mozharovskyi, and R. Dyckerhoff. Depth and depth-based classification with R-package ddalpha. *Journal of Statistical Software, Articles*, 91(5):1–46, 2019.

[62] K. Ramsay, S. Durocher, and A. Leblanc. Integrated rank-weighted depth. *Journal of Multivariate Analysis*, 173:51–69, 2019.

[63] E. Rio. *Asymptotic Theory of Weakly Dependent Random Processes*. Springer, 2017.

[64] M. Sart. Estimation of the transition density of a markov chain. *Annales de l’Institut Henri Poincaré (B) Probability and Statistics*, 50(3):1028–1068, 2014.

[65] X. Shi, Y. Zhang, and Y. Fu. Two-sample tests based on data depth. *Entropy*, 25(2), 2023. ISSN 1099-4300. doi: 10.3390/e25020238.

[66] G. Staerman, P. Mozharovskyi, and S. Clémenccon. The area of the convex hull of sampled curves: a robust functional statistical depth measure. In *International Conference on Artificial Intelligence and Statistics*, pages 570–579. PMLR, 2020.

[67] I. Steinwart and A. Christmann. Fast learning from non-i.i.d. observations. *NIPS*, pages 1768–1776, 2009.

[68] I. Steinwart, D. Hush, and C. Scovel. Learning from dependent observations. *Journal of Multivariate Analysis*, 100(1):175–194, 2009.

[69] J. W. Tukey. Mathematics and the picturing of data. In *Proceedings of the International Congress of Mathematicians, Vancouver, 1975*, volume 2, pages 523–531. Canadian Mathematical Congress, 1975.

[70] A. van der Vaart. *Asymptotic Statistics*. Cambridge University Press, 1998.

[71] Y. Vardi and C.-H. Zhang. The multivariate l_1 -median and associated data depth. *Proceedings of the National Academy of Sciences*, 97(4):1423–1426, 2000.

[72] Y. Zuo and R. Serfling. Structural properties and convergence results for contours of sample statistical depth functions. *The Annals of Statistics*, 28(2):483–499, 2000.

[73] Y. Zuo and R. Serfling. General notions of statistical depth function. *The Annals of Statistics*, 28(2):461–482, 2000.

Supplementary Material

The Supplementary Material is organized into two main parts:

1. Part A: Provides some mathematical background, examples, and detailed technical proofs of the results presented in the main article.
2. Part B: Offers expanded descriptions of experiments from Section 4 of the main text, along with additional numerical experiments not included in the final article due to space limitations.

A Technical appendix

A1 Statistical Depths of Multivariate Probability Distributions

In this section, we will describe some of the well known multivariate statistical depth functions and we state the validity of the properties (P1)-(P6') described in section 2.1

A1.1 Halfspace depth The halfspace depth (HD), introduced by [69], is the first and most widely known example of a multivariate depth function. For a point $x \in E$ and a probability distribution $P \in \mathcal{P}(\mathcal{B}(E))$, $D_P(x)$ is defined as infimum of the measures, according to P , of the halfspaces containing x , that is

$$HD_P(x) = \inf_{u \in \mathbb{S}_{d-1}} \{P(\mathcal{H}_{u,x})\}.$$

where $\mathcal{H}_{u,x} = \{y \in \mathbb{R}^d : \langle u, y - x \rangle \geq 0\}$ for all $(u, x) \in \mathbb{S}_{d-1} \times E$.

The validity of the properties (P1) to (P2) for all $P \in \mathcal{P}(\mathcal{B}(E))$ was proved in Theorem 2.1 of [73], while the property (P5) was established in Lemma 6.1 in [24]. Regarding (P6), Theorem A.3 of [57] shows that it holds for all probability measures, P such that $P(L) = 0$ for all hyperplanes $L \subset E$. Property (P6'') trivially holds for $\mathcal{A} = \{H : H \text{ open half-spaces of } \mathbb{R}^d\}$.

The computational complexity of calculating the halfspace depth presents several challenges. It has been established that determining the exact HD of a single point in arbitrary dimensions, based on sample of n points, is NP-hard, as shown in [38]. Several algorithms have been proposed for the exact computation of HD , with a computational complexity of $O(n^{d-1} \ln n)$. See for instance [50] and [29] for a compendium on this subject. To address this issue, various approximation algorithms have been proposed, for example, [14] developed a Monte Carlo approximation algorithm to treat the problem in high dimensions while approximation procedures using random projections have been explored in [28, 20, 58]. A compendium of additional approximation efforts can be found in the introduction of [58].

A1.2 Simplicial depth In [47], the concept of *simplicial depth* (SD) was introduced. It is defined as the probability that a point $x \in E$ is contained inside a random simplex whose vertices are $d + 1$ independent observations from a probability distribution P .

$$SD_P(x) = \mathbb{P}\{x \in S(X_1, \dots, X_{d+1})\}.$$

where X_1, \dots, X_{d+1} is a random sample from P and $S(x_1, \dots, x_{d+1})$ is the d -dimensional simplex with vertices x_1, \dots, x_{d+1} .

For general distributions, the simplicial depth satisfies (P1), (P2) and (P5) [47, Theorems 1 and 2]. If P is absolutely continuous and angularly symmetric, then SD also satisfies (P3) and (P4). However, for general discrete distributions, it fails to satisfy (P3) and (P4) (see counterexamples 1, 2 and 3 in [73]).¹ Similarly to the halfspace depth, if the P -measure of all hyperplanes is zero, then SD also satisfies (P6) [30, Corollary 2]. Property (P6'') has been shown to be valid for $\mathcal{A} = \{\cap_{i=1}^d H_i : H_1, \dots, H_d \text{ open half-spaces of } \mathbb{R}^d\}$, see Dümbgen [30, Theorem 1].

The most general algorithm for computing SD for a d -dimensional point given a sample of n points, has a computational complexity of $O(n^{d+1})$, as described in [15], and it is believed that the bound can not be improved to less than $O(n^{d-1})$. In [2] it has been shown that computing the simplicial depth exactly is $\#P$ -complete and $W[1]$ -hard if the dimension is part of the input.

¹In [12], a different definition for SD was proposed. This one works for the counterexamples shown by [73] and reduces to the original SD in the continuous case. However, it still does not satisfy (P3) and (P4) for general discrete distributions.

A1.3 Lens depth Let x_1 and x_2 be two points in E and let $\|\cdot\|$ be a norm in E . The lens $L(x_1, x_2)$ of x_1 and x_2 is defined as the intersection of the closed balls with radius $\|x_1 - x_2\|$, and centered at x_1 and x_2 . Figure 4 illustrates this region in \mathbb{R}^2 $L(x_1, x_2)$ when using the Euclidean norm.

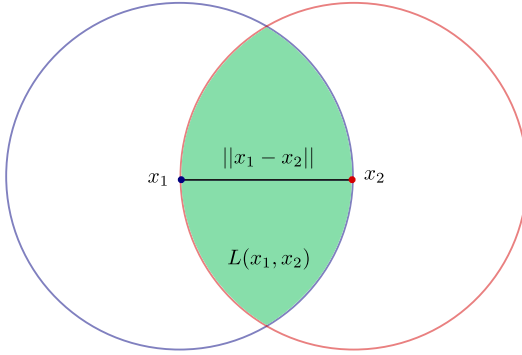


Figure 4: Graphical representation of the region $L(x_1, x_2)$ in \mathbb{R}^2 using the Euclidean norm.

Using the concept of lens and inspired by the spherical depth, previously introduced in [31], [51] defined the *lens depth* (*LD*) of a point $x \in E$ and a probability $P \in \mathcal{P}(\mathcal{B}(E))$ as the probability that x belongs to the random lens $L(X_1, X_2)$, where X_1 and X_2 are two independent random vectors sample from P , this is

$$LD_P(x) = P\{x \in L(X_1, X_2)\}.$$

Theorem 1 in [51] shows that *LD* satisfies a variation of (P1), that is, *LD* is affine invariant when using the Mahalanobis distance and orthogonally invariant when using the Euclidean distance on E . Theorem 2 of the same paper established the validity of (P2). Examples 1, 2 and 3 in [34] show that, like in the Simplicial depth, properties (P3) and (P4) are not satisfied in general. Regarding the continuity properties, Sections 3.3 and 3.4 in [34] established the validity of (P5) and (P6') for all $P \in \mathcal{P}(\mathcal{B}(E))$ such that $P(\|X_1 - X_2\| = \max\{\|X_1 - x\|, \|X_2 - x\|\}) = 0$ for all $x \in E$.

The main advantage of the lens depth, besides its easy interpretation, is that the computational efficiency of its sampled version is $O(n^2)$ [55, pp. 22].

A1.4 Mahalanobis depth Given a d -dimensional distribution P with expectation μ_P and covariance matrix Σ_P , the Mahalanobis norm of $x \in \mathbb{R}^d$ with respect to P is defined as $\|x\|_{\Sigma_P}^2 = x^T \Sigma_P^{-1} x$. This norm, introduced in [52], and the distance defined by it, measures the distance between the point x and the distribution P . Using this concept, the Mahalanobis depth is defined as:

$$MD_P(x) = (1 + \|x - \mu_P\|_{\Sigma_P}^2)^{-1}.$$

The Mahalanobis depth satisfies properties (P1) through (P5) for general distributions. Additionally, for distributions with a regular covariance matrix, it also satisfies (P6). Regarding the computation of its sampling version, the execution times are virtually independent of (moderate values of) n and d (the actual complexity being $O(n)$). For a detailed description of this depth as well as the properties it satisfies, see [55].

A2 The Topology \mathcal{T} on the Space \mathbb{T} of Finite Length Paths

In order to facilitate the exposure, we will concentrate on the case $d = 1$. The properties in the case $d > 1$ follow directly from the natural isomorphism between $(\mathbb{R}^d)^n$ and \mathbb{R}^{dn} for $n \geq 1$.

Denote by \mathbb{R}^∞ the *space of finite sequences over \mathbb{R}* , that is

$$\mathbb{R}^\infty = \{(x_1, x_2, \dots) \in \mathbb{R}^{\mathbb{N}} : \text{all but finitely many } x_i \text{ equal } 0\},$$

For every $n \in \mathbb{N}$, let $\text{In}_{\mathbb{R}^n} : \mathbb{R}^n \rightarrow \mathbb{R}^\infty$ denote the canonical inclusion $\text{In}_{\mathbb{R}^n}(x_1, \dots, x_n) = (x_1, \dots, x_n, 0, 0, \dots)$. The images of these inclusions are $\text{In}_{\mathbb{R}^n}(\mathbb{R}^n) = \mathbb{R}^n \times \{(0, 0, \dots)\}$. Therefore, $\mathbb{R}^\infty = \bigcup_{n=1}^{\infty} \text{In}_{\mathbb{R}^n}(\mathbb{R}^n)$. This allows us to identify each $\text{In}_{\mathbb{R}^n}(\mathbb{R}^n)$ with its corresponding \mathbb{R}^n and \mathbb{T} with \mathbb{R}^∞ . Endow each \mathbb{R}^n with its natural Borealian

topology $\mathcal{B}(\mathbb{R}^n)$. The finite topology \mathcal{T} , also called the *weak topology induced by $\{\mathcal{B}(\mathbb{R}^n)\}_{n \in \mathbb{N}}$* [27, pp. 131], is defined as follows :

$$\mathcal{T} = \{U \subset \mathbb{T} : U \cap \mathbb{R}^n \in \mathcal{B}(\mathbb{R}^n) \ \forall n \in \mathbb{N}\}.$$

The following proposition resumes the main topological properties of the space $(\mathbb{T}, \mathcal{T})$. These results can be found in sections VI.8 and A.4 in [27].

PROPOSITION A2.1. (PROPERTIES OF \mathcal{T}) *The following properties hold true for \mathcal{T} .*

- (i) *The space $(\mathbb{T}, \mathcal{T})$ is complete.*
- (ii) *Each \mathbb{R}^n , as a subspace of $(\mathbb{T}, \mathcal{T})$, retains its original topology $\mathcal{B}(\mathbb{R}^n)$.*
- (iii) *If (Y, \mathcal{Y}) is a topological space, then, a function $f : \mathcal{T} \rightarrow Y$ is continuous if and only if, for all $n \in \mathbb{N}$, the restriction $f \circ \text{In}_{\mathbb{R}^n}$ is continuous as a function of $(\mathbb{R}^n, \mathcal{B}(\mathbb{R}^n))$ to (Y, \mathcal{Y}) .*
- (iv) *If $\{x_m\}_{m \in \mathbb{N}}$ converges to $x = (x_1, \dots, x_n)$ in $(\mathbb{T}, \mathcal{T})$, then there exists M such that $x_m \in \mathbb{R}^n$ for all $m \geq M$ and $x_m \rightarrow x$ in $\mathbb{R}^n, \mathcal{B}(\mathbb{R}^n)$.*
- (v) *\mathcal{T} is smallest topology that makes all the inclusions $\text{In}_{\mathbb{R}^n}$ continuous (i.e. $(\mathbb{T}, \mathcal{T})$ is a coherent space).*

A direct consequence of part (iii) of Proposition A2.1 is that a set $K \subset \mathbb{T}$ is compact if and only if, for all $n \in \mathbb{N}$, $K \cap \mathbb{R}^n$ is compact in $\mathcal{B}(\mathbb{R}^n)$. We will say that a sequence $\{\mathbf{x}_n\}_{n \in \mathbb{N}}$ of elements of \mathbb{T} *goes to infinity* when there exist $m, M \in \mathbb{N}$ such that $\mathbf{x}_n \in \mathbb{R}^m$ for all $n \geq M$ and the sequence $\{\mathbf{x}_n\}_{n \geq M}$ goes to infinity in $\mathcal{B}(\mathbb{R}^m)$ (i.e. $\{\|\mathbf{x}_n\|\}_{n \geq M}$ goes to infinity with n .)

A3 On Markov Kernel Inference

A kernel Π is said to admit a density with respect to the measure λ if there is a non-negative function π defined in $E \times E$ such that for all $x \in E$ and $A \in \mathcal{B}(E)$ we have

$$\Pi(x, A) = \int_A \pi(x, y) d\lambda(y).$$

For kernels that admit a density, the subject of the non-parametric estimation of the kernel Π has received considerable attention in the literature. A popular method to build an estimator of π is to divide an estimator of the joint density of (X_i, X_{i+1}) by an estimator of the density of X_i . The resulting estimator is called a quotient estimator. Due to its simplicity, the most popular of them is the *Nadaraya-Watson* estimator, defined as

$$(A3.1) \quad \pi_n(x, y) = \frac{\sum_{i=0}^{n-1} h_n^{-1} K(h_n^{-1}(x - X_i)) K(h_n^{-1}(y - X_{i+1}))}{\sum_{j=0}^{n-1} K(h_n^{-1}(x - X_j))},$$

where h_n is a bandwidth parameter and $K : E \rightarrow \mathbb{R}$ is a measurable function that satisfies the following conditions:

- $|K|$ is bounded.
- $\|x\| |K(x)| \rightarrow 0$ as $\|x\| \rightarrow \infty$.
- $\int_E |K(x)| dx = 1$.

Theorem 1 in [6] shows that if $nh_n^2 \rightarrow 0$, \mathbf{X} is positive recurrent and its invariant probability has density f , then, for every $x \in E$ such that $f(x) > 0$ and f is continuous at x we have that $\pi_n(x, y)$ converges in probability to $\pi(x, y)$ for all $y \in E$. Under slightly stronger assumptions, the same paper showed that the estimator is asymptotically normal. It was shown to be strongly consistent in [25], while Berry-Essen type inequalities were obtained in [7].

In addition to the Nadaraya-Watson estimator, various other estimators have been suggested in the literature. These include wavelet-based estimators [17], regression-based estimators [43], and projection-based estimators [44], among others. For these type of estimators, minimax-rates have been obtained as well as bounds for the integrated quadratic risk. For a detailed review of this subject, see [64].

A3.1 Estimating the cumulative distribution function When $E \subset \mathbb{R}$, for x fixed, integrating over y in equation (A3.1), and letting $G(t) := \int_{-\infty}^t K(t) dt$ we get the following consistent estimator $\hat{F}_x(y)$ of the cumulative distribution function of $X_1|X_0 = x$

$$(A3.2) \quad \hat{F}_x(y) = \frac{\sum_{i=0}^{n-1} K(h_n^{-1}(x - X_i))G(h_n^{-1}(y - X_{i+1}))}{\sum_{j=0}^{n-1} K(h_n^{-1}(x - X_j))},$$

therefore, the distribution function \hat{F}_x can be written as a weighted sum of the distribution functions $G(h_n^{-1}(y - X_{i+1}))$

A4 On the Symmetry property

In this section, we discuss the property of maximality at path of centers of the Markovian depth, showing an example of where it holds. We also discuss the concept of symmetry centers, and we provide an example that shows why a property like (P3) is not useful in the Markovian scenario.

A4.1 Maximality at path of centers Consider the case where $d = 1$ and the Markovian depth function $D_{\Pi}(\mathbf{x})$ is based on Tukey's half-space depth. In this situation, we have: $\forall (x, y) \in \mathbb{R}^2$ (c.f. [21, pp. 754])

$$(A4.3) \quad D_{\Pi_x}(y) = \min \{ \Pi_x((-\infty, y]), 1 - \Pi_x((-\infty, y)) + \Pi_x(\{y\}) \}.$$

Assume that for all $x \in \mathbb{R}$, the distribution Π_x is continuous and non-degenerate. Then for each $x \in \mathbb{R}$, there is a unique $\theta(x) \in \mathbb{R}$ such that $\Pi_x((-\infty, \theta(x)]) = 1/2$. The point $\theta(x)$ has maximal Tukey's depth of $1/2$ with respect to the distribution Π_x . As a result, the Markov depth attains its maximum value of $1/2$ at the path $(x_0, \theta(x_0), \dots, \theta^{(n-1)}(x_0))$ for any $n \geq 1$ and $x_0 \in \mathbb{R}$.

The following example shows that this situation is quite common.

EXAMPLE A4.1. (MARKOV CHAIN WITH CONTINUOUS MARGINALS) Suppose that Π admits a non-constant density function $f(x, t)$ with respect to the Riemann's integral, that is

$$\Pi(x, (-\infty, y]) = \int_{-\infty}^y f(x, t) dt \quad \forall x, y \in \mathbb{R}.$$

Then, the distribution functions of Π_x are all continuous and non-degenerated, therefore their Markovian depth is maximal at path $(x_0, \theta(x_0), \dots, \theta^{(n-1)}(x_0))$ for any $n \geq 1$ and $x_0 \in \mathbb{R}$.

Many well-known Markov models have densities, for example Random Walks, Autoregressive processes and Random coefficient autoregressive models. For more examples and a detailed description, see [26, Chapter 2].

A4.2 Symmetry centers A natural way to define symmetry with respect to the null trajectory $\mathbf{0}$ (i.e. the infinite path with all components equal to 0) in the Markov space is by requiring that for all $n \in \mathbb{N}$ and any Borel set $A \subset \mathbb{R}^{n+1}$, we have: $\mathbb{P}\{(X_0, \dots, X_n) \in A\} = \mathbb{P}\{(X_0, \dots, X_n) \in -A\}$, where $-A = \{\mathbf{x} = (x_0, \dots, x_n) \in \mathbb{R}^{n+1} \text{ s.t. } (-x_0, \dots, -x_n) \in A\}$.

The following example shows a Markov chain that fulfills this symmetry definition, but where the null trajectory is unrealizable.

EXAMPLE A4.2. (UNREALIZABLE SYMMETRIC PATH) Consider the Simple Symmetric Random walk. This chain is defined as $X_0 = 0$, $X_{n+1} = X_n + \epsilon_n$ for $n \geq 0$ with $\{\epsilon_n\}_{n \geq 0}$ being an i.i.d. sequence of random variables such that $\mathbb{P}(\epsilon_n = 1) = \mathbb{P}(\epsilon_n = -1) = 1/2$. This model is symmetric w.r.t the infinite null trajectory $\mathbf{0}$, however, this trajectory is unrealizable, as $\mathbb{P}(X_{n+1} = X_n) = 0$ for all n .

A5 Examples of Markov Depths

In this section we show the form of the Markovian depth in some scenarios. The main result in this section is Example A5.3.

EXAMPLE A5.1. (MARKOV TUKEY'S DEPTH IN \mathbb{R}) Suppose \mathbf{X} is a Markov chain with kernel Π taking values in $E \subseteq \mathbb{R}$. Let $\mathbf{x} = (x_0, \dots, x_n) \in \mathbb{T}$ be such that Π_{x_i} is a continuous random variable for $i = 0, \dots, n - 1$. Then, the Markov depth D_{Π}^H , based on the halfspace depth has the form

$$(A5.4) \quad D_{\Pi}^H(\mathbf{x}) = \sqrt[n]{\prod_{i=1}^n \min \{ \Pi_{x_{i-1}} ((-\infty, x_i]), 1 - \Pi_{x_{i-1}} ((-\infty, x_i]) \}}.$$

The next example shows that the simplicial depth can also be written in a simple closed form.

EXAMPLE A5.2. (SIMPLICIAL TUKEY'S DEPTH IN \mathbb{R}) Under the same conditions of Example A5.1 we have that the the Markov depth D_{Π}^S , based on the simplicial depth, is written as

$$(A5.5) \quad D_{\Pi}^S(\mathbf{x}) = \sqrt[n]{\prod_{i=1}^n \Pi_{x_{i-1}} ((-\infty, x_i]) (1 - \Pi_{x_{i-1}} ((-\infty, x_i]))}.$$

Building on the previous examples, we now show the main result of this section, that is, the form of the sampling versions of the Markovian depth for real valued Markov chains with densities. We borrow the notation from section A3.

EXAMPLE A5.3. (SAMPLING VERSIONS IN \mathbb{R}) Let \mathbf{X} be a real valued, positive recurrent valued Markov chain with kernel Π , having continuous density π . Suppose we have a realization $X = (X_0, \dots, X_n)$ of \mathbf{X} , and let $\mathbf{x} = (x_0, \dots, x_m) \in \mathbb{T}$. Under this hypothesis, the Nadaraya-Watson estimator (A3.2), based on X can be used, and the estimators $\hat{F}_{x_{i-1}}(y)$ of the marginal CDFs are continuous as a function of y . Then, by examples A5.1 and A5.2, the sampling versions D_{Π}^H of the Markov depths D_{Π}^H and D_{Π}^S adopt the form:

$$D_{\Pi}^H(\mathbf{x}) = \sqrt[m]{\prod_{i=1}^m \min \{ \hat{F}_{x_{i-1}}(x_i), 1 - \hat{F}_{x_{i-1}}(x_i) \}} \quad , \quad D_{\Pi}^S(\mathbf{x}) = \sqrt[m]{\prod_{i=1}^m \hat{F}_{x_{i-1}}(x_i) (1 - \hat{F}_{x_{i-1}}(x_i))},$$

where

$$\hat{F}_{x_{i-1}}(x_i) = \frac{\sum_{k=0}^{n-1} K(h_n^{-1}(x_{i-1} - X_k)) G(h_n^{-1}(x_i - X_{k+1}))}{\sum_{k=0}^{n-1} K(h_n^{-1}(x_{i-1} - X_k))},$$

and K and G are as defined in (A3.2). Notice that the dimensions of the sample X and the point \mathbf{x} do not necessarily coincide.

Our final example shows the form of the Markovian depth based on the Rank-Weighted (IRW) depth.

EXAMPLE A5.4. (MARKOV IRW-DEPTH) Recently, in order to avoid optimization issues, various alternatives to Tukey's depth functions have been proposed, see e.g. [21]. In [62] (see also [19] for a variant guaranteeing the affine-invariance property), a new data depth, referred to as the Integrated Rank-Weighted (IRW) depth, is defined by substituting an integral over the sphere \mathbb{S}^{d-1} for the infimum. When based on the IRW-depth, the Markov depth is given by: $\forall n \geq 1, \forall \mathbf{x} = (x_0, \dots, x_n) \in E^{n+1}$,

$$D_{\Pi}(\mathbf{x}) = \sqrt[n]{\prod_{i=1}^n \int_{u \in \mathbb{S}_{d-1}} \Pi_{x_{i-1}}(\mathcal{H}_{u,x_i}) \omega_{d-1}(du)},$$

where ω_{d-1} is the spherical probability measure on \mathbb{S}_{d-1} . The main advantage of the IRW depth is of computational nature, the integrals w.r.t. ω_{d-1} involved in (A5.4) can be approximated by Monte Carlo procedures: $Z/||Z|| \sim \omega_{d-1}$ as soon as $Z \sim \mathcal{N}(0, \mathcal{I}_d)$ is a standard centered Gaussian.

A6 Technical Proofs

The proofs of the theoretical results stated in the paper are detailed below.

A6.1 Proof of Proposition 3.1 As we \mathbb{P}_ν almost-surely have: $\forall n \geq 1$,

$$D_\Pi(X_0, \dots, X_n) = \exp \left(\frac{1}{n} \sum_{i=1}^n \log(D_{\Pi_{X_{i-1}}}(X_i)) \right),$$

the result straightforwardly follows from the SLLN and the CLT for additive functionals of aperiodic Harris recurrent Markov chains (refer to *e.g.* Theorem 4.1 in [40]), combined with the delta method (applied to the differentiable function $x \mapsto \exp(x)$ (see *e.g.* Theorem 3.1 in [70]). The asymptotic variance is given by

$$(A6.6) \quad \sigma_\Pi^2 = \int_{(x,y) \in E^2} \log^2(D_{\Pi_x}(y)) \mu d(x) \Pi_x(dy) - \int_{x \in E} \left(\int_{y \in E} \log(D_{\Pi_x}(y)) \Pi(x, dy) \right)^2 \mu(dx).$$

A6.2 Proof of Theorem 3.1

Independence from the initial law: This property follows directly from definition 3.2 as the Markovian sample path depth is defined in terms of the transition probability kernel only.

Affine invariance: Let $f(x) = Ax + b$ be an affine invariant transformation. From the definition 3.2, it is clear that if we show $D_{f(\Pi)f(y_0)}(f(y_1)) = D_{\Pi_{y_0}}(y_1)$ for all, $y_0, y_1 \in E$ then the claim of the theorem follows immediately.

Denote by F_{y_0} the distribution of $f(Y)$, where Y is a random variable with distribution Π_{y_0} . The affine invariance of D implies that

$$(A6.7) \quad D_{F_{y_0}}(f(y_1)) = D_{\Pi_{y_0}}(y_1).$$

On the other hand, notice that, for any $C \in \mathcal{B}(E)$ and $y \in E$ we have

$$f(\Pi)(y, C) = \mathbb{P}(f(X_1) \in C | f(X_0) = y) = \Pi(f^{-1}(y), f^{-1}(C)),$$

therefore, $f(\Pi)_{f(y_0)}(C) = \Pi(y_0, f^{-1}(C)) = \Pi_{y_0}(f^{-1}(C)) = F_{y_0}(C)$, which shows that the distributions F_{y_0} and $f(\Pi)_{f(y_0)}$ coincide. The result now follows from (A6.7).

Vanishing at infinity: Before proving the main result, we need the following lemma.

LEMMA A6.1. *Let $\mathbf{x} = (x_0, \dots, x_m) \in E^{m+1}$. For any $\epsilon > 0$, if there is j such that $D(x_j, \Pi_{x_{j-1}}) < \epsilon$, then $D_\Pi(\mathbf{x}) < \epsilon^{1/m}$.*

Proof. [Proof of Lemma A6.1] Using that D is always between 0 and 1 we have $\sqrt[m]{\prod_{i=1}^m D_{\Pi_{x_{i-1}}}(x_i)} \leq \epsilon^{1/m}$. \square

Let $\{\mathbf{x}_n\}_{n=1}^\infty \subset \mathbb{T}$ be a sequence that tends to infinity in \mathcal{T} . The topology of the torus implies that there exists an integer m such $\mathbf{x}_n \in E^{m+1}$ for n big enough and that $\|\mathbf{x}_n\|_\infty := \max_{0 \leq i \leq m} \|x_{i,n}\|$ tends to infinity with n . Suppose that $D_\Pi(\mathbf{x}_n)$ does not converge to 0, then, there is an $\epsilon > 0$ such that $D_\Pi(\mathbf{x}_n) > \epsilon$ for all n . Therefore, by the contrapositive of Lemma A6.1, for all $n \in \mathbb{N}$ and $i = 0, \dots, m$ we have $D_{\Pi_{x_{i-1,n}}}(x_{i,n}) > \epsilon^m$.

Because $D_{\Pi_{x_0}}$ satisfies (P2), we have that there exists C_1 such that $D_{\Pi_{x_0}}(y) < \epsilon^m$ for all y with $\|y\| > C_1$, therefore, $\|x_{1,n}\| \leq C_1$ for all n . By the same reasoning, but using that $\sup_{\|x\| \leq C_1} D_{\Pi_x}(y) \rightarrow 0$ as $\|y\| \rightarrow \infty$, we obtain that there exists C_2 such that $\|x_{2,n}\| \leq C_2$ for all n . Repeating the same argument for $i = 2, \dots, m$, we get that the sequences $\{x_{2,n}\}_{n \geq 1}, \dots, \{x_{m,n}\}_{n \geq 1}$ are all bounded, therefore $\|\mathbf{x}_n\|_\infty$ is also bounded, which contradicts our assumption that $\|\mathbf{x}_n\|_\infty$ tends to infinity.

A6.3 Proof of Proposition 3.2 This is a direct consequence of the monotonicity of the exponential and logarithmic functions.

A6.4 Proof of Theorem 3.2

Continuity in \mathbf{x} : If \mathbf{x}_n is a sequence in \mathbb{T} that converges to \mathbf{x} , then $\mathbf{x}_n \in E^{m+1}$ for n big enough. Moreover, $\mathbf{x}_n = (x_{0,n}, \dots, x_{m,n})$ converges to $\mathbf{x} = (x_0, \dots, x_m)$ in E^{m+1} if and only if $x_{i,n} \rightarrow x_i$ in E for $i = 1, \dots, m$. Notice that for each $i = 1, \dots, m$ and n big enough we have

$$|D_{\Pi_{x_{i-1,n}}}(x_{i,n}) - D_{\Pi_{x_{i-1}}}(x_i)| \leq |D_{\Pi_{x_{i-1,n}}}(x_{i,n}) - D_{\Pi_{x_{i-1}}}(x_{i,n})| + |D_{\Pi_{x_{i-1}}}(x_{i,n}) - D_{\Pi_{x_{i-1}}}(x_i)|.$$

The first term on the right hand side of the previous inequality tends to 0 as n tends to infinity thanks to property (P6) of D and the weakly convergence of $\Pi_{x_{i-1},n}$ to $\Pi_{x_{i-1}}$. Similarly, the second term goes to 0 as n goes to infinity in virtue of (P5). This shows that $D_{\Pi_{x_{i-1},n}}(x_{i,n}) \rightarrow_n D_{\Pi_{x_{i-1}}}(x_i)$ for $i = 1, \dots, m$. The continuity of D_Π now follows from (3.2) and the continuity of the function $y \mapsto \sqrt[n]{y}$.

Continuity in Π : For each $\mathbf{x} \in \mathbb{T}$ we have

$$|D_{\Pi^{(n)}}(\mathbf{x}) - D_\Pi(\mathbf{x})| \leq \max_{0 \leq i \leq m-1} |D_{\Pi_{x_i}^{(n)}}(x_{i+1}) - D_{\Pi_{x_i}}(x_i+1)|,$$

the result now follows from (P6').

A6.5 Proof of Theorem 3.3

We will prove the following stronger version of Theorem 3.3

THEOREM A6.1. *Let $n \geq 1$ and $\mathbf{x} = (x_0, \dots, x_n) \in E^{n+1}$. Consider two transition probabilities Π and $\hat{\Pi}$ on E . Suppose that D fulfills property (P6'') and $C_d \|\Pi_{x_i} - \hat{\Pi}_{x_i}\|_{\mathcal{A}} < \min\{D_{\Pi_{x_i}}(x_{i+1}), D_{\hat{\Pi}_{x_i}}(x_{i+1})\}$ for $i = 1, \dots, n$. Then,*

$$(A6.8) \quad |D_\Pi(\mathbf{x}) - D_{\hat{\Pi}}(\mathbf{x})| \leq \frac{7}{4} C_d \frac{D_\Pi(\mathbf{x})}{H_{\Pi, \hat{\Pi}}(\mathbf{x})} \max_{i=0, \dots, n-1} \|\Pi_{x_i} - \hat{\Pi}_{x_i}\|_{\mathcal{A}},$$

where

$$H_{\Pi, \hat{\Pi}}(\mathbf{x}) := \frac{n}{\sum_{i=0}^{n-1} \frac{1}{\sqrt{D_{\Pi_{x_i}}(x_{i+1}) D_{\hat{\Pi}_{x_i}}(x_{i+1})}}}$$

represents the harmonic mean of $\sqrt{D_{\Pi_{x_i}}(x_{i+1}) D_{\hat{\Pi}_{x_i}}(x_{i+1})}$, $i = 0, \dots, n-1$.

Proof. [Proof Theorem A6.1] Let $h_i = D_{\hat{\Pi}_{x_i}}(x_{i+1}) - D_{\Pi_{x_i}}(x_{i+1})$, then, we can write $\ln D_{\hat{\Pi}_{x_i}}(x_{i+1}) = \ln D_{\Pi_{x_i}}(x_{i+1}) + \ln(1 + h_i/D_{\Pi_{x_i}}(x_{i+1}))$ and

$$(A6.9) \quad |D_\Pi(\mathbf{x}) - D_{\hat{\Pi}}(\mathbf{x})| = D_\Pi(\mathbf{x}) \left| 1 - \exp \left(\frac{1}{n} \sum_{i=0}^{n-1} \ln \left(1 + \frac{h_i}{D_{\Pi_{x_i}}(x_{i+1})} \right) \right) \right|.$$

By (P6'') and our hypothesis, we have $|h_i| \leq C_d \|\Pi_{x_i} - \hat{\Pi}_{x_i}\|_{\mathcal{A}} < \min\{D_{\Pi_{x_i}}(x_{i+1}), D_{\hat{\Pi}_{x_i}}(x_{i+1})\}$ for $i = 0, \dots, n-1$, therefore, $|h_i|/\min\{D_{\Pi_{x_i}}(x_{i+1}), D_{\hat{\Pi}_{x_i}}(x_{i+1})\} < 1$ for all i . Using the inequality $|\ln(1+t)| \leq |t|/\sqrt{1+t}$, valid for $t \geq -1$ [10, pp. 160], and the fact that $(h_i/D_{\Pi_{x_i}}(x_{i+1}))(1 + h_i/D_{\Pi_{x_i}}(x_{i+1}))^{-1} = h_i/D_{\hat{\Pi}_{x_i}}(x_{i+1})$, we obtain

$$(A6.10) \quad \left| \ln \left(1 + \frac{h_i}{D_{\Pi_{x_i}}(x_{i+1})} \right) \right| \leq \frac{|h_i|}{\sqrt{D_{\Pi_{x_i}}(x_{i+1}) D_{\hat{\Pi}_{x_i}}(x_{i+1})}}, \quad i = 0, \dots, n-1$$

which is smaller than 1. Therefore, $|\frac{1}{n} \sum_{i=0}^{n-1} \ln(1 + h_i/D_{\Pi_{x_i}}(x_{i+1}))| < 1$. This allows us to apply the inequality $|1 - e^t| < \frac{7}{4}|t|$ (valid for $|t| < 1$) [10, pp. 82] on equation (A6.9), which combined with equation (A6.10) shows that

$$|D_\Pi(\mathbf{x}) - D_{\hat{\Pi}}(\mathbf{x})| \leq \frac{7}{4} D_\Pi(\mathbf{x}) \frac{1}{n} \sum_{i=0}^{n-1} \frac{|h_i|}{\sqrt{D_{\Pi_{x_i}}(x_{i+1}) D_{\hat{\Pi}_{x_i}}(x_{i+1})}}.$$

Equation (A6.8) now follows from (P6''). \square

Now we proceed to the proof of Theorem 3.3. First, notice that if $C_d \|\Pi_{x_i} - \hat{\Pi}_{x_i}\|_{\mathcal{A}} \geq \min\{D_{\Pi_{x_i}}(x_{i+1}), D_{\hat{\Pi}_{x_i}}(x_{i+1})\}$ for some i , then $C_d \max_{i=0, \dots, n-1} \|\Pi_{x_i} - \hat{\Pi}_{x_i}\|_{\mathcal{A}} > \epsilon$, which implies that the right hand side of (3.5) is bigger than $\frac{7}{4} D_\Pi(\mathbf{x})$. In this case, the inequality is trivially satisfied because $D_\Pi(\mathbf{x})$ and $D_{\hat{\Pi}}(\mathbf{x})$ are both between 0 and 1. On the other hand, when $C_d \|\Pi_{x_i} - \hat{\Pi}_{x_i}\|_{\mathcal{A}} < \min\{D_{\Pi_{x_i}}(x_{i+1}), D_{\hat{\Pi}_{x_i}}(x_{i+1})\}$ for all i , we can apply Theorem A6.1. Equation (3.5) now follows from equation (A6.9) using that $\sqrt{D_{\Pi_{x_i}}(x_{i+1}) D_{\hat{\Pi}_{x_i}}(x_{i+1})} \geq \min\{D_{\hat{\Pi}_i}(x_{i+1}), D_{\Pi_i}(x_{i+1})\} > \epsilon$.

B Additional Numerical Experiments

This appendix provides detailed numerical experiments where we show the practical utility of the Markov depth concept introduced in this paper. Section B1 expands on the anomaly detection examples presented in Section 4, describing the process in detail as well as presenting additional results. In Section B2 we present Markovian DD-plots, a visualization technique useful for clustering, while Section B3 shows an example of how to use the Markov depth for homogeneity testing.

All the experiments presented in this section and in the main text were executed in an Apple M2 computer with 16 GB of RAM running MacOS 14.2.1 and Python 3.10.8. All the code is available in https://github.com/statsmarkov/depth_markov.

B1 Unsupervised Detection of Anomalous Paths

In this subsection we provide additional details on the simulation study from Section 4, including results omitted from the main text due to space limitations.

B1.1 Description of the models Nonlinear time-series. For our first example, we borrow a model from Econometrics. In order to replace the assumption of constant volatility with the much more realistic conditional volatility in econometric models, [32] introduced the Autoregressive Conditional Heteroskedasticity (ARCH) model. This model recognizes that past financial data influences future data, allowing the conditional variance to change over time as a function of past errors, while leaving the unconditional variance constant. This model has been used since the 1980s to model the returns of financial assets ([8]).

For simplicity, in our study we will consider the ARCH(1) model (studied in [37, 33]).² If we denote by X_n the quantity of interest at time n , then the ARCH(1) model is defined as $X_{n+1} = m(X_n) + \sigma(X_n) + \epsilon_n$ where $m : \mathbb{R} \mapsto \mathbb{R}$ and $\sigma : \mathbb{R} \mapsto \mathbb{R}_+^*$ are unknown measurable non-negative functions and ϵ_n is a sequence of i.i.d. random variables with mean 0 and variance 1 independent of X_0 . Notice that in this model, $\mathbb{E}[X_{n+1}|X_n] = m(X_n)$ and $\text{Var}(X_{n+1}|X_n) = \sigma^2(X_n)$. For our simulations we have chosen $m(x) = (1 + \exp(-x))^{-1}$ and $\sigma(x) = \psi(x + 1.2) + 1.5\psi(x - 1.2)$ where $\psi(x)$ is the density function of a standard normal distribution and ϵ_n is a sequence of i.i.d. standard normal variables.

Queuing system. In our second example, we will consider a GI/G/1 queuing model with interarrival times T_n and service times V_n where $\{T_n\}_{n \geq 0}$ and $\{V_n\}_{n \geq 0}$ are independent sequences of random variables. Denote by X_n the waiting time of the n -th customer and assume that $X_0 = 0$ (*i.e.* the first customer is immediately served). Example 6.1 in [5] shows that $X_{n+1} = \max(0, X_n + W_n)$, where $W_n = V_n - T_n$. If the there are random variables V and T such that $T_n \sim T$ and $V_n \sim V$ for all n , then this model corresponds to the *Modulated random walk on the half line* (MRW-HL) described in Example 2.1, namely, $U(x, (-\infty, y]) = F(y)$ where F is the distribution function of $V - T$. Notice that, in this case, $\Pi(x, [0, y]) = F(y - x)$ for all $x, y \geq 0$. For our simulation study, we have chosen V and T as exponential distributions with expectations 0.45 and, 0.5 respectively.

B1.2 Anomaly generation This section provides a detailed description of the process used to generate the anomalies for each model.

Nonlinear time-series. We generated four types of anomalies for the ARCH(1) model, which are illustrated in Figure 5 and described in detail below.

- **Isolated anomaly (Shock):** We randomly select an integer t between 1 and $k - 3$, then, we generate 3 trajectories: the first one is a regular trajectory of size t , the second one (of size 2) is generated from a ARCH(1) model with $m(x) = 5x$ and $\sigma(x) = \sqrt{|x|}$ and the third one is a regular trajectory of length $k - t - 2$. The anomalous path is then conformed by joining the 3 trajectories.
- **Dynamic anomaly I (Perturbed mean):** We follow an approach similar to previous one, but here the second trajectory has length equal of $\lfloor 0.6k \rfloor$ and is generated from an ARCH(1) model with $m(x) = (2 + \exp(-x))^{-1}$ and the same σ as the regular one.

²The original model described by [32] is the ARCH(1) model with $m(x) = 0$ and $\sigma(x) = \sqrt{\alpha_0 + \alpha_1 x^2}$ where α_0 and α_1 are positive constants.

- **Dynamic anomaly II (Increasing volatility):** The method is the same as in the preceding anomaly, but using the same mean as in the regular trajectory and taking $\sigma(x) = 0.5\sqrt{x^2 + 1}$. Contrary to the normal one, the conditional variance in this case is increasing (as a function of $|x|$).
- **Shift anomaly (Deterministic mean):** Similar to the others, but with deterministic mean (equal to 2) and the same variance as the regular one.

Queuing system. The four type of anomalies used in study of the queuing model were generated as described below. A graphical representation of these anomalies is presented in Figure 6.

- **Isolated anomaly (Shock) :** We randomly select an integer t between 1 and $\lfloor 0.9k \rfloor$, then, we generate 3 trajectories: the first one is a regular trajectory of size t , the second one (of size $\lfloor 0.1k \rfloor$) is generated from a queuing model with V as an exponential distribution with mean 2.25 and same interarrival times as the original model (*i.e.* the server takes, on average, 5 more time to complete a task). The third one is a regular trajectory of length $\lfloor 0.9k \rfloor - t$, that starts from 0. The anomalous path is then conformed by joining the 3 trajectories. This anomaly simulates a temporary malfunction in the server, causing the waiting time of the customers to increase very fast.
- **Dynamic anomaly I (Faster arrivals):** We follow an approach similar to the shock anomaly, but here the second trajectory has length equal of $\lfloor 0.2k \rfloor$ and is generated from an MRW-HL model where the interarrival times have exponential distribution with mean 0.1. This simulates a period of increased customer arrivals.
- **Dynamic anomaly II (Slower service times):** This method is the same as in the previous anomaly, but the anomalous trajectory has length equal to $\lfloor 0.2k \rfloor$ and we take $V = 0.55\mathcal{U}$ where \mathcal{U} has uniform distribution between 0 and 2 and using the same interarrival times as in the regular model. Notice that for the anomalous part, $\mathbb{E}V - \mathbb{E}T = 0.05$, hence, this part of the trajectory is not positive recurrent, although the divergence is very slow. It simulates a temporary decrease in the performance of the server.
- **Shift anomaly (Deterministic arrivals):** Similar to the previous anomalies, but the anomalous path length is 25, and we take $T_n = 2^{-n}$, V as in the regular model, and constructing the third trajectory starting from the last point of the second trajectory. This simulates a situation where, during a period of time, the number of customers increases very fast and after this spike ends the server does not restart.

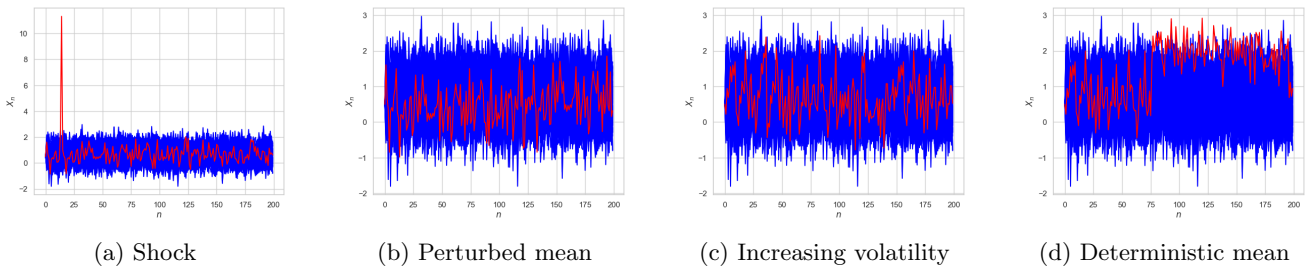


Figure 5: Examples of anomalies in ARCH(1) model. Blue lines represent regular trajectories while red lines represent anomalous trajectories.

B1.3 Results For each model, we generated a long training path ($n = 1000$) and four contaminated datasets. Each contaminated dataset consisted of 200 paths with lengths varying between 50 and 200, where half of the paths contained a specific type of anomaly. We computed a kernel estimator $\hat{\Pi}$ using the long training path. This estimator was then used to calculate the Markov depth D_{Π} , based on Tukey's depth, for each trajectory in the contaminated datasets.

The results (see Table 1 in the main text) indicate that the Markov depth detects with very high accuracy classic anomalies such as shocks/shifts, while it is also capable of detecting with high accuracy the dynamic anomalies studied. The corresponding ROC curves in Figures 7 and 8 reveal its strong performance on the different types of anomaly considered.

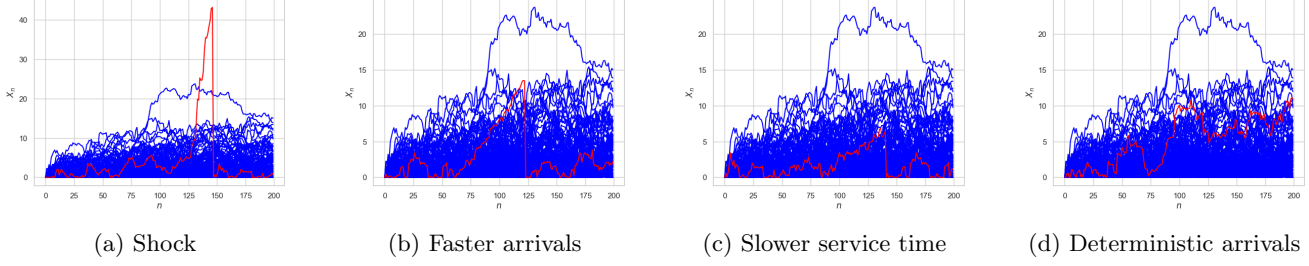


Figure 6: Examples of anomalies in the MRW-HL model. Blue lines represent regular trajectories while red lines represent anomalous trajectories.

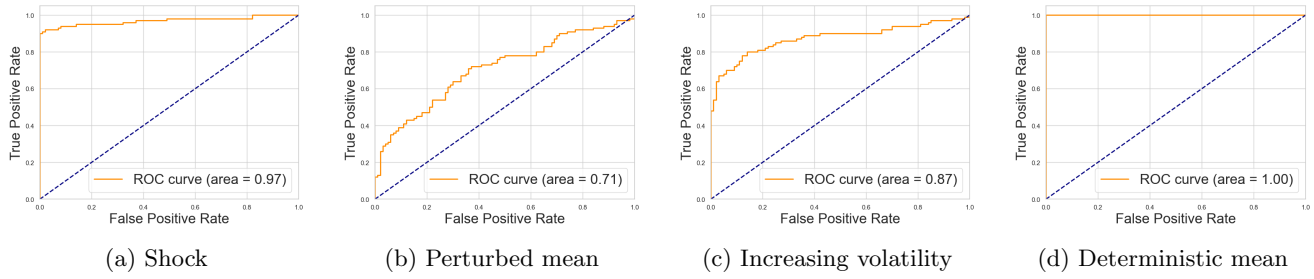


Figure 7: ROC curves of the studied anomalies in the ARCH(1) model.

B1.4 Comparison with competitors In order to compare our proposal (D_{Π}) against the most commonly used methods for anomaly detection in multivariate data, specifically Isolation Forest (IF), Local Outlier Factor (LOF), and Mahalanobis Depth (MD), we must limit our analysis to scenarios where all trajectories are of equal length. For this experiment, we generated 8 datasets (one for each type of anomaly and model), each containing 100 trajectories of 200 points, with 5% of the trajectories exhibiting a specific type of anomaly. We then applied our method alongside the previously mentioned anomaly detection algorithms to each dataset. For IF and LOF we have used the implementation contained in the python library *sklearn* [60], while for the Mahalanobis depth we have used the Python package *data-depth*,³ all parameters used in the algorithms were set to their default values. For our Markovian depth algorithm, we generated a sample of 10 trajectories of size 200 in order to obtain an estimator of the kernel. The ROC curves (figures 9 and 10) and the AUC (table 2) clearly show that, for classical anomalies (shock and shift) our method performs similarly to the best between IF, LOF and MD, while for dynamic anomalies, it outperforms it.

Table 2: Comparison of the AUC for different classifiers in the ARCH(1) and queuing models.

Anomaly type	ARCH(1) model				Queuing model			
	IF	LOF	MD	D_{Π}	IF	LOF	MD	D_{Π}
Shock	0.75	0.82	0.68	0.85	0.67	0.98	0.44	0.98
Dynamic anomaly I	0.42	0.63	0.52	0.84	0.59	0.80	0.80	0.94
Dynamic anomaly II	0.68	0.90	0.91	0.99	0.64	0.55	0.50	0.85
Shift	1	1	0.6	1	0.93	0.99	0.69	0.98

³Available at <https://data-depth.github.io>

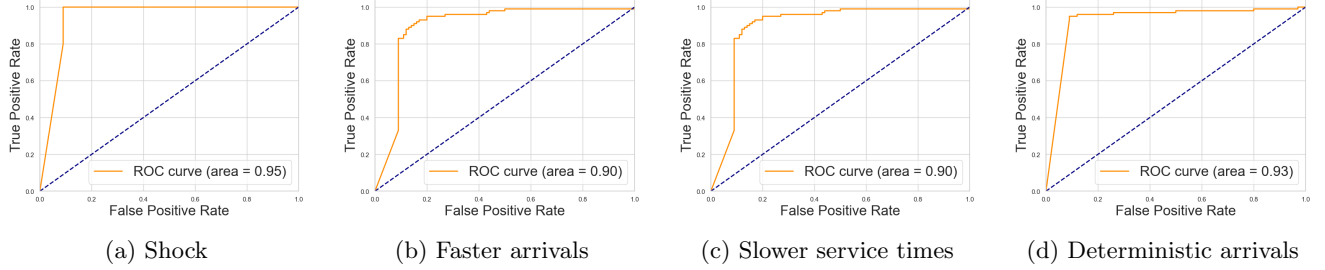


Figure 8: ROC curves of the studied anomalies in the queuing model.

B2 Clustering Markov Paths

The infinite dimension of Markov chains makes it challenging to visualize the data and understand the underlying structure. As it was shown in Figures 1a, 5 and 6, even in the case $d = 1$ and constant path length, plotting the paths as a function of n is not very useful, as the trajectories tend to occupy a vast part of the space due to the ergodicity.

Markovian depth functions can be effectively utilized to develop a visual diagnostic tool for Markovian paths, building upon the Depth vs. Depth plot (DD-plot), first introduced in [49] for multivariate data. For two sets of Markov trajectories $\mathcal{X} = \{\mathbf{x}_1, \dots, \mathbf{x}_{n_1}\}$ and $\mathcal{Y} = \{\mathbf{y}_1, \dots, \mathbf{y}_{n_2}\}$ with corresponding kernel estimators $\hat{\Phi}$ and $\hat{\Psi}$, the Markovian DD-plot is obtained by plotting in the Euclidean plane the points

$$\{(D_{\hat{\Phi}}(\mathbf{x}), D_{\hat{\Psi}}(\mathbf{x})) : \mathbf{x} \in \mathcal{X} \cup \mathcal{Y}\}.$$

To illustrate the use of DD-plots, we will revisit the ARCH(1) model described in section B1.1. Recall that in that model $m(x) = (1 + \exp(-x))^{-1}$ and $\sigma(x) = \psi(x + 1.2) + 1.5\psi(x - 1.2)$ where $\psi(x)$ is the density function of a standard normal distribution. We have generated 5 data sets, each one containing 50 trajectories of random lengths (between 50 and 200 steps). Each one of these datasets, labeled $\mathcal{X}, \mathcal{Y}_a, \mathcal{Y}_b, \mathcal{Y}_c, \mathcal{Y}_d$, is constructed following an ARCH(1) model with the parameters stated in Table 3. Figure 11, shows the DD-plots of \mathcal{X} (blue points) and \mathcal{Y}_i (yellow stars) for $i = a, b, c, d$.

It can be readily seen that, the more “similar” the distributions of both sets (in the sense of the parameters used to generate the data) are, the more commingled the points in the DD-plot are. Notice that the samples in \mathcal{Y}_a have the same distribution as the samples in \mathcal{X} , hence, it is expected that the DD-plot shows a straight line, see 11a. Conversely, the more the distributions diverge, the more separated the points (see Figure 11d).

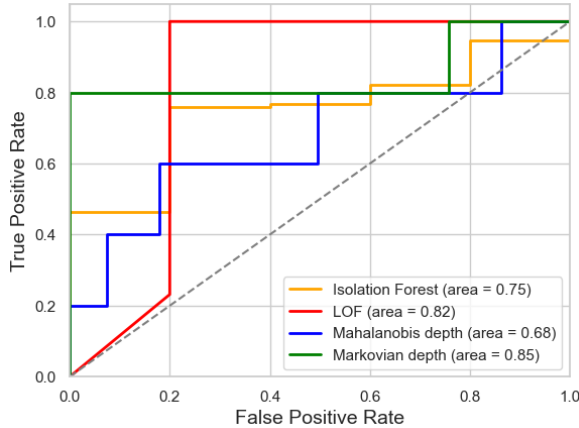
Table 3: Parameters of the ARCH(1) model used in Figure 11

Dataset	$m(x)$	$\sigma(x)$
\mathcal{X}	$(1 + \exp(-x))^{-1}$	$\psi(x + 1.2) + 1.5\psi(x - 1.2)$
\mathcal{Y}_a	$(1 + \exp(-x))^{-1}$	$\psi(x + 1.2) + 1.5\psi(x - 1.2)$
\mathcal{Y}_b	$(2 + \exp(-x))^{-1}$	$\psi(x + 1.2) + 1.5\psi(x - 1.2)$
\mathcal{Y}_c	$(4 + \exp(-x))^{-1}$	$\psi(x + 1.2) + 1.5\psi(x - 1.2)$
\mathcal{Y}_d	$(1 + \exp(-x))^{-1}$	1

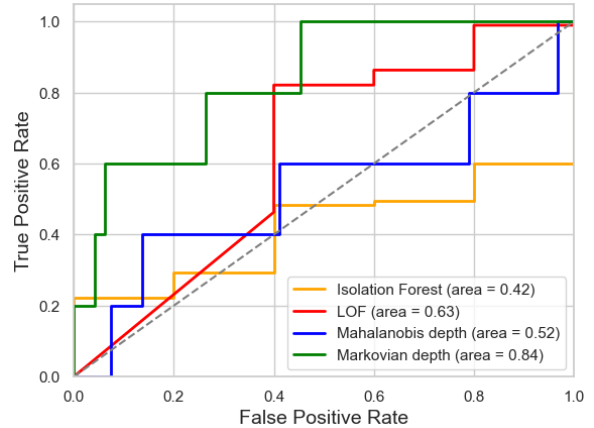
B3 Homogeneity Testing

The proposed Markovian depth can further be used to provide a formal inference, which we exemplify as a nonparametric test of homogeneity between the distribution of two Markov chains. To do this, we will use the depth-based Wilcoxon rank-sum test, proposed in [48].

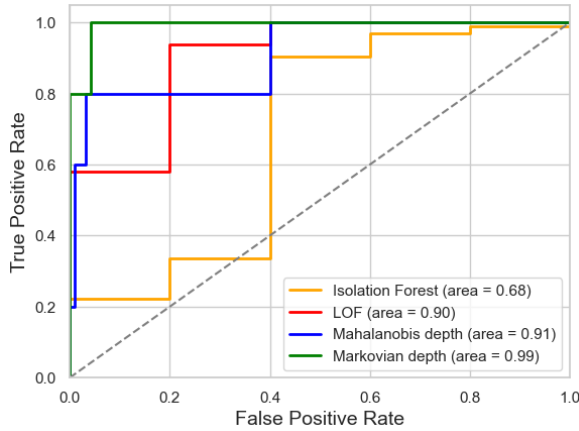
Consider two ARCH(1) models, one with $m(x) = (1 + \exp(-x))^{-1}$ and $\sigma(x) = \psi(x + 1.2) + 1.5\psi(x - 1.2)$, and the other with $m(x) = (1 + \alpha + \exp(-x))^{-1}$ and the same σ as the first one. For different values of α , ranging from



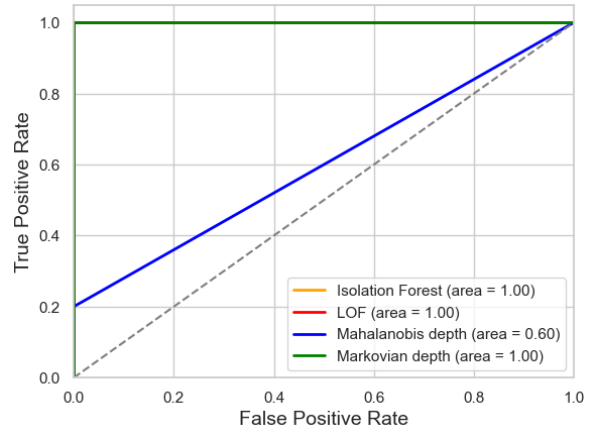
(a) Shock



(b) Perturbed mean (Dyn. an. II)



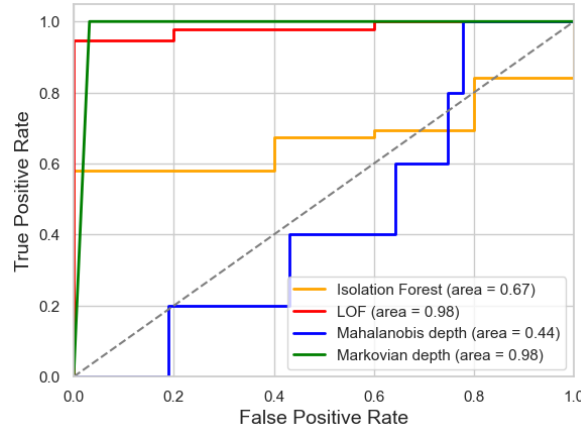
(c) Increasing volatility (Dyn. an. II)



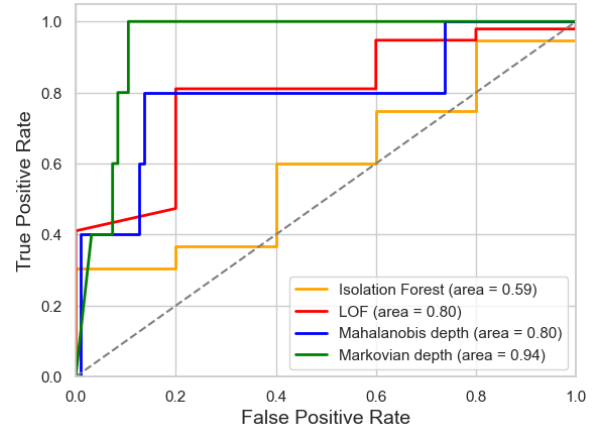
(d) Deterministic mean (Shift)

Figure 9: ROC curves for each type of anomaly in the ARCH(1) model.

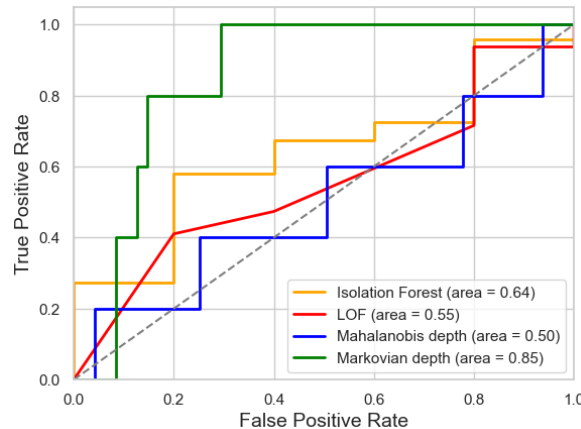
0.3 (very similar distributions) to 1 (reasonably different) we perform the aforementioned depth-based Wilcoxon rank-sum test, generating 50 trajectories of random length (between 50 and 200) for each chain and using a reference trajectory of length 1000 from the first chain. Figure 12 presents the p -values of the test for each α , averaged over 50 repetitions. The p -values effectively identify the differences between the two distributions when they exist.



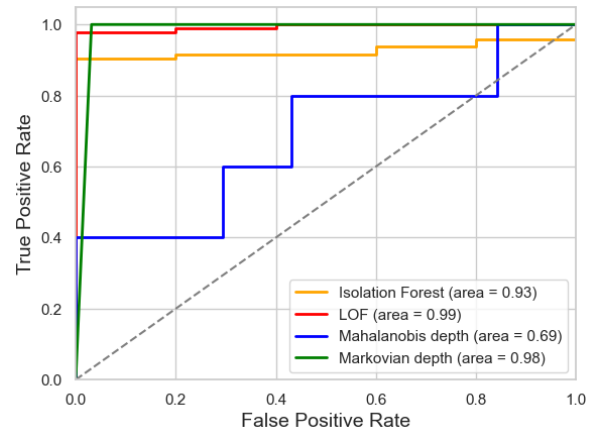
(a) Shock



(b) Faster arrivals (Dyn. an. I)

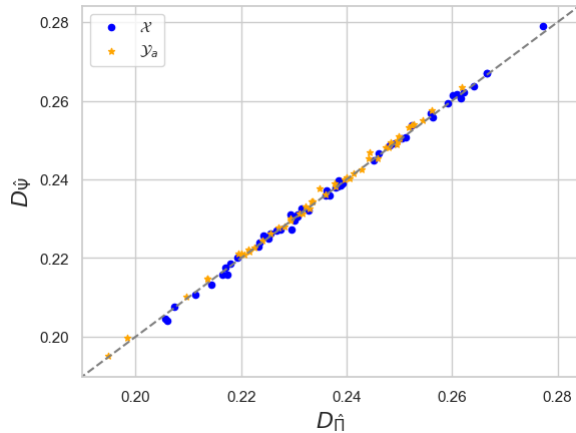


(c) Slower services (Dyn. an. II)

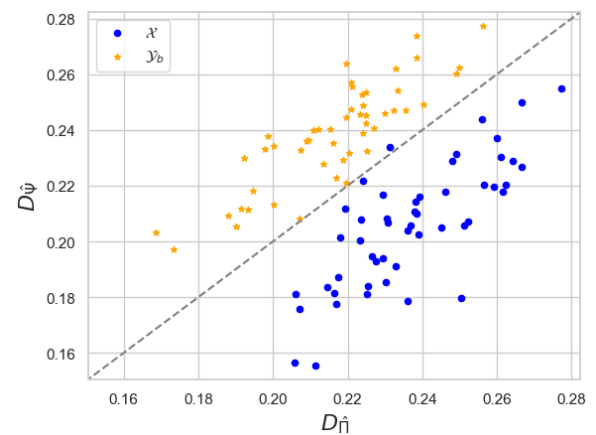


(d) Deterministic arrivals (Shift)

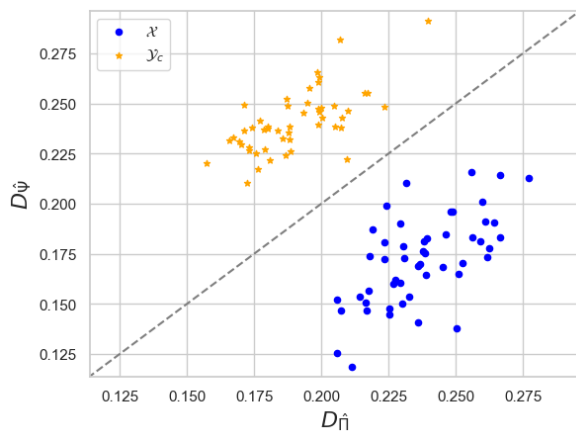
Figure 10: ROC curves for each type of anomaly in the queuing model.



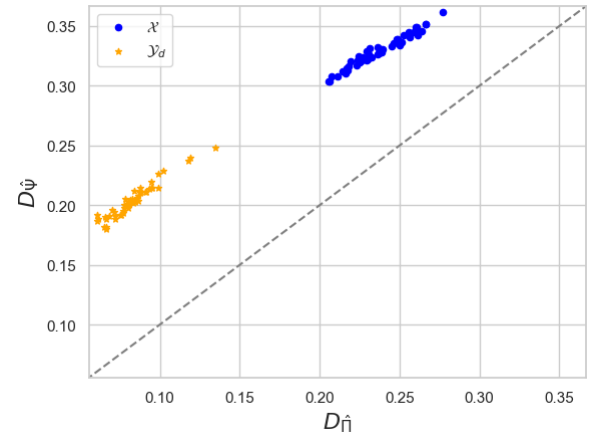
(a)



(b)



(c)



(d)

Figure 11: Markovian DD-plots for ARCH(1) models with parameters described in Table 3.

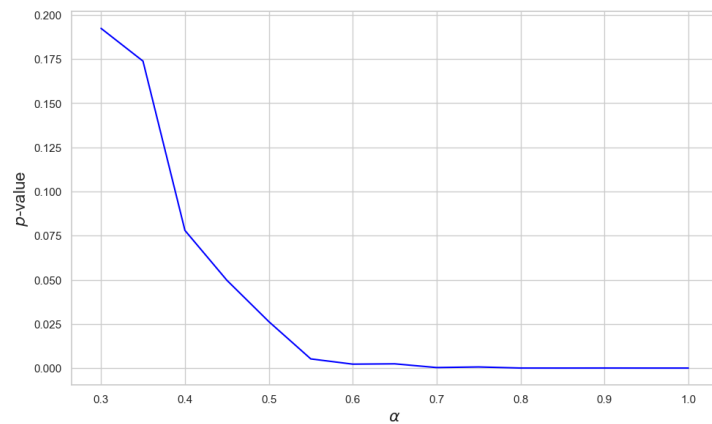


Figure 12: Average p -values (as a function of α) for the homogeneity test.